

A General Form for Continuous Variable Quantum Kernels

L. J. Henderson^{1,2}, R. Goel¹, and S. Shrapnel^{1,2}

¹*School of Mathematics and Physics, The University of Queensland, QLD 4072, Australia and*

²*ARC Centre for Engineered Quantum Systems, The University of Queensland, QLD, 4072, Australia.*

(Dated: January 12, 2024)

The popular qubit framework has dominated recent work on quantum kernels, with results characterising expressability, learnability and generalisation. As yet, there is no comparative framework to understand these concepts for continuous variable (CV) quantum computing platforms. In this paper we represent CV quantum kernels as holomorphic functions and use this representation to provide several important theoretical insights. The approach permits a general closed form solution for all CV quantum kernels and shows every such kernel can be expressed as the product of Gaussian and polynomial terms. Furthermore, it enables quantification of a quantum-classical separation for all such kernels via a notion of “stellar rank”, and provides intuition for how bandwidth hyper-parameter tuning results in trades-off between learnability and efficient classical simulability.

I. INTRODUCTION

The quantum machine learning (QML) community has recently begun to explore whether quantum resources may be useful for kernel machine learning [1–4]. While research has typically focused on improving traditional classical kernel methods, such as support vector machines, classical kernelisation is in fact far more ubiquitous. Kernels appear as filters in convolutional neural networks [5], can represent attention matrices in transformer networks [6], are used as training signals for generative networks [7], and can provide a key mechanism for causal discovery [8]. Clearly, there is much to be gained by understanding whether quantum kernels can provide an advantage over their classical counterparts [9–13].

This recent exploration has led to the development of quantum kernel selection tools [14], generalisation bounds [15], optimal solution guarantees [1, 16], and has resulted in several physical implementations [17–20]. The community has learned that although entangled quantum kernels—including those generated by deep parametrised quantum neural networks (PQNN)—are highly expressive, such expressivity typically comes at a cost. This is the so-called “exponential concentration” problem, analogous to the barren plateau problem in quantum neural networks [21]—as quantum kernels become more expressive, they typically also become exponentially harder to learn and less likely to generalise [22–24]. Essentially, the value of the kernel between different datapoints decreases as a function of the size of the problem—for discrete variable quantum kernels, a highly expressive kernel yields exponential concentration. Recent numerical work suggests it may nonetheless be possible to overcome these learning difficulties by manipulating a bandwidth hyper-parameter to tune the expressibility of the quantum kernel [25, 26], a technique inspired by bandwidth tuning of classical Gaussian kernels [27]. Finding the sweet spot where the quantum kernel is both learnable and generalisable, but is nonetheless still classically hard to simulate is, however, an open challenge [28]. Robustness to noise also presents a further unexplored challenge to such kernel tuning techniques.

As a consequence, the QML community has to some extent converged on a new quest. Rather than seeking a quantum advantage for kernel machine learning *per se*, physicists are now searching for inductive biases that specific quantum kernels, or families of quantum kernels, may bring to particular ML tasks [23]. The thinking is inspired by the tremendous advantage convolutional neural networks have provided imaging tasks due to their translational invariance [5]. To this end, the group theoretic structure of some specific quantum kernels has been used to exploit structure in certain classical learning problems in order to prove quantum advantage [17, 18, 29]. As such, there is strong motivation to identify and understand new classes of quantum kernels.

An outstanding key challenge to substantial progress is the theoretically opaque nature of quantum kernels. While classical kernels employ the “kernel trick” — one avoids explicitly evaluating the kernel in feature space by using an analytic representation acting in the original data space (e.g. the Gaussian function) — quantum kernels evaluate inner products directly in feature space via measurement expectation values that approximate each kernel matrix entry up to some additive error. Analytic forms are rarely available and thus theoretical understanding of quantum kernels is somewhat limited.

Interestingly, almost all the work on quantum kernels to date has focussed on discrete, finite dimensional quantum systems, such as those generated by parameterised quantum circuits. While a few works have evaluated specific, continuous variable, infinite dimensional quantum encodings [2, 30–33], there is as yet no unifying approach to CV quantum kernels.

In this paper we examine continuous variable quantum kernels through the lens of holomorphic functions. This

allows us to present a framework with a very natural taxonomy of kernel “quantumness”, achieved via the notion of stellar rank. Stellar rank ultimately provides useful guarantees as to the hardness of classical simulation [34, 35]. Furthermore, the holomorphic representation permits insight into the general theoretical structure of CV quantum kernels—every kernel can be expressed as the product of a Gaussian and polynomial term, where the polynomial degree scales with the stellar rank ($4n$). This structure permits some preliminary intuition into possible tradeoffs between bandwidth hyperparameter tuning (to improve generalisation and learnability) and consequent loss of quantum advantage [28], and also hints at how exponential concentration and noise will manifest in CV quantum kernels.

The paper is organised as follows: in section II we introduce relevant mathematical notation and background. In section III we review holomorphic representations of quantum CV systems (based on [35]). In section IV we formalise how one may define a holomorphic quantum kernel and show it satisfies necessary properties. Section V is split into 4 subsections, presenting a displaced Fock state encoding, displacement-phase encoding, general CV encoding and general qudit encoding. It is here we show that all kernels are expressed as a Gaussian times a polynomial. While for particular CV quantum kernels there are simpler analytic forms, our goal here is to highlight the general form and characterise their stellar rank. Additionally, we explore the notion of bandwidth and how it affects our kernels. We conclude with section VI, where we discuss findings and make suggestions for future work.

II. PRELIMINARIES

Here we fix notation and formalise the necessary mathematics.

A. Notation:

Vectors are denoted in bold unless otherwise specified (e.g. \mathbf{x}) as are matrices, the latter with capital letters only (e.g. \mathbf{X}). Sets and vector spaces are written in mathematical calligraphic font (e.g. \mathcal{X}). Complex numbers will be stated explicitly or as 2-dimensional real vectors, most commonly we use z . Conjugates of complex vectors or matrices are written with superscript asterisk (e.g. \mathbf{x}^*). Overlines instead represent completion of sets, e.g. $\overline{\mathcal{X}}$.

$|\psi\rangle$ will always be a quantum state. We reserve n for the Fock state number of such a quantum state. We write all kernels using k , whether they are quantum or classical will be made explicit within the text. We define \mathcal{N}_0 is the set of natural numbers including 0.

Hypergeometric functions are written as ${}_iF_j$, with i, j representing the specific form. Polynomials of x are written as $P(x)$ and Gaussians as $G(x)$. As usual, Γ is the gamma function:

$$\Gamma(z) = \int_0^\infty dt \, t^{z-1} e^{-t} \quad (1)$$

for $\text{Re}(z) > 0$ and $(b)_j$ is the Pochhammer symbol

$$(b)_j := \frac{\Gamma(b+j)}{\Gamma(b)}.$$

The inner product of a specific Hilbert space, \mathcal{H} , is written as $\langle \mathbf{x} | \mathbf{x}' \rangle_{\mathcal{H}}$. Unless otherwise specified, the norm $\|\mathbf{x}\|_{\mathcal{H}}$ is given by $\sqrt{\langle \mathbf{x} | \mathbf{x} \rangle_{\mathcal{H}}}$ where \mathcal{H} is the space in which \mathbf{x} has a well defined inner product.

We define holomorphic functions, denoted by F^* , as complex functions which are complex differentiable in a neighbourhood about every point. $F_{\mathbf{x}}^*$ is a holomorphic function dependent on some classical data $\mathbf{x} \in \mathcal{X}$. Stellar functions are a subset of holomorphic functions with finite roots and written as the product of a polynomial and Gaussian term. As n is used as our Fock state number, our stellar rank (the number of complex roots of F^*) is also n .

B. Kernel Machine Learning

The core tenet of kernel machine learning (ML) is the application of linear statistical methods to complex, non-linear data. The data—while not separable in the original data space—can be linearly separated after transformation into a higher dimensional space. The key advantage from kernel methods is the use of the ‘kernel trick’, where one does not need to explicitly compute the data embedding. This trick has found its way into many applications such as ML classification, regression, and clustering [27].

For simplicity, we will describe the supervised learning case as described in [30] to provide the necessary background. We are given some labelled dataset, $\{(\mathbf{x}_k, y_k), k = 1, \dots, M\}$ and aim to find a mapping $f(\mathbf{x})$ for some new unlabeled data point, where $f(\mathbf{x})$ is determined by some structure, pattern or probability distribution within the data. The solution to this learning problem is given by,

$$f^*(\mathbf{x}) = \arg \min_{h \in \mathcal{H}} \frac{1}{M} \sum_{i=1}^M \mathcal{L}(h(\mathbf{x}_i), y_i) + g(\|h\|), \quad (2)$$

where we define \mathcal{L} as the loss function characterising the performance of the learned function and \mathcal{H} is the Hilbert space of learning functions we are considering [36]. $g(\cdot)$ is a monotonically increasing regularisation function which penalises overfitting, favouring a smooth function with better generalisation.

The crucial step in kernel methods is the encoding of data. Given some data from a space \mathcal{X} we define a data mapping into a Hilbert space \mathcal{H} by a non-linear feature map $\Phi : \mathcal{X} \rightarrow \mathcal{H}$. We usually take the feature map such that the data is not linearly separable in \mathcal{X} but is in \mathcal{H} —commonly achieved by taking \mathcal{H} to be a higher dimension than \mathcal{X} . One such kernel using this mapping is,

$$k(\mathbf{x}, \mathbf{x}') = |\langle \Phi(\mathbf{x}) | \Phi(\mathbf{x}') \rangle_{\mathcal{H}}|^2. \quad (3)$$

k uses the inner product in our feature space to form a measure of similarity between data. We consider the kernel to be symmetric (for real valued kernels, taking the absolute value squared is hence unnecessary) and positive semi-definite, i.e., $\forall \mathbf{x}_i \in \mathcal{X}$ and any $c_i \in \mathbb{C}^n$

$$\sum_{i,j} c_i c_j^* k(\mathbf{x}_i, \mathbf{x}_j) \geq 0. \quad (4)$$

Associated to every such feature space is a unique Reproducing Kernel Hilbert Space (RKHS). This is a space of functions that can be constructed as the completion of the span of kernels,

$$\mathcal{H}_{RKHS} = \overline{\text{span}}\{h_{\mathbf{x}_i} = k(\mathbf{x}_i, \cdot) | \mathbf{x}_i \in \mathcal{X}\}, \quad (5)$$

and includes the reproducing kernel, also known as the evaluation functional, $h_{\mathbf{x}}$, which maps some element of the RKHS $h_{\mathbf{x}_i}$ to $h_{\mathbf{x}_i}(\mathbf{x}) = k(\mathbf{x}_i, \mathbf{x})$. The construction of the RKHS permits a solution to equation 2 given by,

$$f^*(\mathbf{x}) = \sum_{\mathbf{x}_i \in \mathcal{X}} c_i k(\mathbf{x}, \mathbf{x}_i), \quad (6)$$

for some $c_i \in \mathbb{R}$ [37].

Formal analysis of classical kernel functions allows one to characterise three key quantities: learnability, expressivity and generalisability. Learnability describes how well the optimal kernel as defined in equation 6 can be found as a function of the size of the problem. Expressivity is used to measure the complexity of problems kernels can linearly classify. If a kernel is universal (i.e. perfectly expressive), it can precisely separate any two given sets from a compact metric space of finite training data [36]. All universal kernels are also characteristic, and can thus be utilised in probabilistic ML applications [38].

Generalisation theory aims to assess the quality of the learning scheme. Generalisation bounds provide a measure of how well the kernel - given some finite dataset from a distribution P - can be applied to randomly sampled data from P that was not in the initial dataset. The boundedness of evaluational functions in any RKHS, $\{f \in RKHS : \|f\| \leq B\}$ yields generalisation bounds given by

$$\mathbb{E}_{\mathbf{x} \in \mathcal{D}} |h^*(\mathbf{x}) - f| \leq \frac{2B}{\sqrt{M}}, \quad (7)$$

where the average is with respect to a fixed distribution \mathcal{D} over the input data. M is the size of the labelled dataset and B is a function of the specific kernel and the loss function from equation 2 [39]. Such approaches are often defined in terms of VC dimension or fat-shattering dimension [40], however, these bounds all represent worst case scenarios

and have limited practical relevance. In practice, bandwidth hyperparameter tuning, which essentially changes the length scale of the kernel, is most often used to improve generalisation. If bandwidth is too small, the kernel will treat most new data points as very far from any training observation, while a bandwidth that is too large creates a kernel that will treat each new data point as nearly equidistant to all training observations. Neither will result in good generalization and clearly bandwidth tuning can have a profound impact on learnability and generalisability. Such tuning is similarly computationally very expensive, although recent techniques utilising Jacobian control have shown some improvement in computational demands [41].

C. Quantum Kernels

Recently, formal similarities between kernel methods and quantum machine learning (QML) methods have become well established [1]. Essentially, QML methods encode data non-linearly into a higher dimensional Hilbert space in which quantum measurement defines a linear decision boundary. For example, in supervised machine learning we can encode our data in the Hilbert space of the quantum system as $x \rightarrow |\Phi(x)\rangle$ and then learn the measurement that optimally separates the data. Typically, this state is prepared with some unitary gate operator $U_\theta(x)$ that acts on the vacuum state $|0 \dots 0\rangle$ such that $U_\theta(x)|0 \dots 0\rangle = |\Phi(x)\rangle$. The kernel function is then defined using the Hilbert-Schmidt inner product as,

$$k(x, x') = |\langle \Phi(x) | \Phi(x') \rangle_{\mathcal{H}}|^2. \quad (8)$$

An important subtlety is that in quantum kernels, we no longer use the same “kernel trick” as in the classical case, kernel entries are not evaluated using a closed form solution applied to the original data space but are rather approximated directly via quantum measurement. This also means that the RKHS of quantum kernels is rarely characterised, though the existence of the quantum feature map directly implies the existence of a RKHS.

While the majority of quantum kernels are characterised using the qubit circuit formalism, several specific examples of CV quantum kernels exist. Maria Schuld’s excellent summary paper includes a description of a coherent state kernel encoding [2] and Tiwari et. al. construct a mathematical representation of coherent quantum kernels using generalised hypergeometric functions [31]. Ghobadi presents a single mode squeezed and a single photon (Fock) state quantum kernel and derives a non-classicality witnesses - a necessary but insufficient condition for quantum advantage - for each [30], and Bowie et. al. describe an experimental platform which exploits Hong–Ou–Mandel interference to evaluate a kernel based on a temporal encoding [33]. There is to date, however, no unifying framework from which to understand these individual results. In the following section we introduce the relevant background to understand our approach.

III. REPRESENTING CONTINUOUS VARIABLE QUANTUM STATES AS HOLOMORPHIC FUNCTIONS

Quantum information processing (QIP) is often separated into two paradigms: discrete variable QIP and continuous variable QIP. The former utilises finite dimensional Hilbert spaces and qubits or qudits, whereas the latter utilises infinite dimensional Hilbert spaces and Bosonic modes. In the discrete case, non-Clifford operations are identified as necessary for bounded error quantum polynomial (BQP) complete, non-classically simulable, computation [42]. Analogously, non-Gaussian operations are identified as necessary for BQP-complete computation in the CV setting [43]. In recent work, Chabaud et. al. present a measure of non-Gaussianity which permits a more nuanced quantification of the computational power of CV quantum computing platforms [34]. In this approach, discrete variable (DV) quantum systems are represented by polynomials while CV ones are fully characterised by holomorphic functions. We will focus on the CV case to generate our main results, but will return to the discrete case in the final section. Holomorphic functions are complex analytic, i.e. they can be written as a complex power series and are complex-differentiable in a neighborhood of each point in their domain. In the CV case, we can decompose a finite rank holomorphic function as a stellar function - a product of a Gaussian and polynomial in z . The polynomial is characterised by its roots and accounts for the non-Gaussianity of the quantum system [34].

For single bosonic modes, with orthonormal basis $\{|n\rangle\}_{n \in \mathbb{N}_0}$, we can encode our state using the canonical coherent states as,

$$|z\rangle_\infty = \sum_{n \geq 0} \frac{z^n}{\sqrt{n!}} |n\rangle. \quad (9)$$

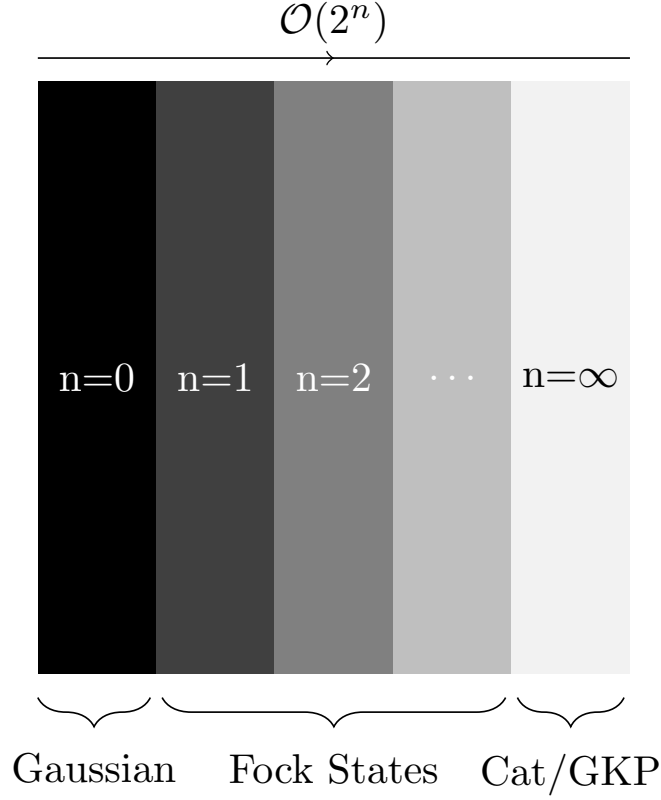


FIG. 1. Adapted from [34]. The taxonomy of stellar functions representing CV quantum states. The $n = 0$ states are classically simulable and include, but are not limited to, coherent states, thermal states, and (multimode) squeezed states. As the stellar rank, n , increases, the strong simulability of the state increases exponentially. The $n = \infty$ states are not part of the Segal-Bargmann (SB) space, but can be arbitrarily approximated by states of finite stellar rank.

One can treat these as phase-space wave functions of a corresponding quantum state.

The following section is adapted from [34], describing the holomorphic framework formalism.

Instead of representing quantum states as infinite countable vectors as seen in the Fock state description, they can be characterized as holomorphic functions through the transformation,

$$|n\rangle \leftrightarrow \left(z \mapsto \frac{z^n}{\sqrt{n!}} \right), \quad (10)$$

for all $n \in \mathbb{N}_0$. Hence a particular quantum state, decomposed into its Fock basis as $|\psi\rangle = \sum_{n \geq 0} \psi^{(n)} |n\rangle$ can be transformed as,

$$|\psi\rangle \leftrightarrow F_\psi^*(z) := \sum_{n \geq 0} \frac{\psi^{(n)}}{\sqrt{n!}} z^n, \quad (11)$$

known as the stellar function of the state $|\psi\rangle$. This stellar function corresponds to an expansion as a sum in the overcomplete basis of Glauber canonical coherent states [34]. Using the Hadamard-Weirstrass factorisation theorem, we can rewrite these stellar functions as

$$F_\psi^*(z) = e^{-\frac{1}{2}az^2 + bz + c} z^k \prod_n \left(1 - \frac{z}{\lambda_n} \right) e^{\frac{z}{\lambda_n} + \frac{1}{2} \frac{z^2}{\lambda_n^2}}, \quad (12)$$

where the constants, $a, b, c, k, \lambda_n \in \mathbb{C}$ are each dependent on $|\psi\rangle$. Here, n is given as the so called stellar rank of the function. For stellar functions of finite rank (i.e. finite roots of the polynomial, n), we can write our function as separable in Gaussian and polynomial functions as,

$$F_\psi^\star(z) = G(z)P(z). \quad (13)$$

This decomposition can be written as,

$$F_\psi^\star(z) = e^{-a/2z^2+bz+c} \sum_{j=0}^N \beta_j z^j, \quad (14)$$

for $a, b, c, \beta_j \in \mathbb{C}$, which is the form that we will use in the remainder of the paper.

These functions live in the Segal-Bargman space, the separable infinite-dimensional Hilbert space of holomorphic functions F^\star over \mathbb{C}^m , satisfying the normalization condition,

$$\|F^\star\|^2 := \int_{\mathbf{z} \in \mathbb{C}^m} d^{2m}z \, e^{-|\mathbf{z}|^2} |F^\star(\mathbf{z})|^2 < +\infty, \quad (15)$$

which constrains $\text{Re}(a) < 2$ in Eq. (14). The SB space has the inner product,

$$\langle F_1^\star | F_2^\star \rangle_{SB} = \int_{\mathbf{z} \in \mathbb{C}^m} d^{2m}z \, e^{-|\mathbf{z}|^2} F_1^\star(\mathbf{z})^* F_2^\star(\mathbf{z}). \quad (16)$$

In the SB space, our operators are functions of the creation and annihilation operators acting on the Hilbert space of our quantum states, and are mapped to differential operators in the SB space by,

$$\hat{a}^\dagger \leftrightarrow z \times \text{ and } \hat{a} \leftrightarrow \partial_z, \quad (17)$$

where $z \times$ acts on a holomorphic function by multiplying it by z and ∂_z takes the partial derivative of it with respect to z . It follows that any unitary evolution acting on an element of the SB space remains within the space. It is also understood that any unitary only changes the polynomial component of a stellar function and Gaussian unitary operations do not change the stellar rank at all.

The stellar functions in this space are described by their stellar rank (n), the number of polynomial roots they have. The key results of [34] and [35] prove that stellar rank provides a useful measure of classical simulability, a fact we later utilise to analyse the simulability of CV quantum kernels. Roughly, the measurement of a general non-separable, CV state ρ can be strongly simulated in time $O(2^n)$, where n is the stellar rank [35].

Common examples of zero stellar rank functions are vacuum states, coherent states, squeezed states and two-mode squeezed states. Fock states of n particle number have stellar rank n , whereas cat states, binomial states, NOON states and GKP states are all infinite stellar rank functions (although, importantly, can be well approximated by functions of finite stellar rank). Important properties of the stellar rank as a measure of non-Gaussianity include the fact that it is conserved under Gaussian operations, that the states of finite stellar rank form a dense subset of the SB space, and that operationally one can climb the hierarchy by acting on a given state with a creation operator (see Figure 1.).

We will next use these representations of CV quantum states to develop analytic representations of CV quantum kernels.

IV. CV QUANTUM FEATURE MAPS

Given some metric space of our data \mathcal{X} we can define our CV holomorphic kernel as follows. Firstly, let us encode our data $\mathbf{x}_i \in \mathcal{X}$ to a quantum state which we then decompose into its Fock basis,

$$\mathbf{x}_i \rightarrow |\psi_{\mathbf{x}_i}\rangle = \sum_{n \geq 0} \psi_{\mathbf{x}_i}^{(n)} |n\rangle. \quad (18)$$

Using the transformation from equation 10 we yield,

$$|\psi_{x_i}\rangle \leftrightarrow F_{x_i}^*(z) := \sum_{n \geq 0} \frac{\psi_{x_i}^{(n)}}{\sqrt{n!}} z^n. \quad (19)$$

This allows our data to be encoded into some continuous variable state via holomorphic functions. This forms our data encoding,

$$x_i \mapsto \phi(x_i) := F_{x_i}^*(z), \quad (20)$$

from which we define our kernel as,

$$k(x_1, x_2) = |\langle \phi(x_1) | \phi(x_2) \rangle|^2 = |\langle F_{x_1}^*(z) | F_{x_2}^*(z) \rangle_{SB}|^2. \quad (21)$$

This function is positive semi-definite and symmetric and thus a valid kernel (see Appendices A and B).

We can define the RKHS as the completion of the span of the kernel function for some data set \mathcal{X} as in equation 5. We see that the Segal Bargmann space can be understood as the RKHS of the Gaussian kernel which itself is universal (appendix C).

V. EXAMPLE CV QUANTUM KERNELS

In order to build some insight into the general form of CV quantum kernels we will first start with some simple examples. We construct an analytic expression for a kernel generated from a single mode, displaced, Fock state encoding and show this kernel is rotationally and translationally invariant, radial and characteristic. We then derive an expression for the same state when one also encodes data into a phase shift—the resulting kernel is no longer translationally or rotationally invariant. Finally, we derive a general closed form solution for any, possibly multi-mode, CV encoded kernel using an arbitrary holomorphic function of stellar rank n .

A. Displacement

We first consider a simple single mode bosonic kernel which encodes data through a general Fock state $|n\rangle$ with an applied displacement unitary $\hat{D}(\alpha)|n\rangle$. To encode 2 pieces of information $\alpha = (\alpha_1, \alpha_2)^\top \in \mathcal{X} \subset \mathbb{R}^2$, we parameterise the displacement operator by the complex number $\alpha := \alpha_1 + i\alpha_2$. This operator acts on any holomorphic function as

$$F^*(z) \mapsto e^{\alpha z - |\alpha|^2/2} F^*(z - \alpha^*). \quad (22)$$

Since displacement is a Gaussian operation, it will not change the stellar rank of $F^*(z)$; therefore the encoded state $\hat{D}(\alpha)|n\rangle$ will have a stellar rank of n . Explicitly, the encoded state is

$$\hat{D}(\alpha)|n\rangle \leftrightarrow F_\alpha^*(z) = e^{\alpha z - |\alpha|^2/2} \frac{(z - \alpha^*)^n}{\sqrt{n!}} \quad (23)$$

and with this encoding, the quantum kernel is

$$k(\alpha, \beta) = |\langle F_\alpha^*(z) | F_\beta^*(z) \rangle|^2 \quad (24)$$

where

$$\begin{aligned} \langle F_\alpha^*(z) | F_\beta^*(z) \rangle &= \int_{z \in \mathbb{C}} d^2 z \, e^{-|z|^2} (F_\alpha^*(z))^* F_\beta^*(z) \\ &= \frac{1}{\pi} \frac{e^{-(|\alpha|^2 + |\beta|^2)/2}}{n!} \int_{z \in \mathbb{C}} d^2 z \, e^{-(|z|^2 - \alpha^* z^* - \beta z)} (z^* - \alpha)^n (z - \beta^*)^n. \end{aligned} \quad (25)$$

After the integration and some algebra (see appendix E for details), we can write down the displacement kernel in closed form as:

$$\begin{aligned}
k_D(\boldsymbol{\alpha}, \boldsymbol{\beta}) &= |\langle F_{\boldsymbol{\alpha}}^*(z) | F_{\boldsymbol{\beta}}^*(z) \rangle|^2 \\
&= \left(\frac{n!}{\pi} \right)^2 e^{-|\boldsymbol{\alpha} - \boldsymbol{\beta}|^2} \left| \sum_{i=0}^n \sum_{j=0}^{n-i} \sum_{k=0}^n \sum_{\ell=0}^{n-k} \sum_{p=0}^{i+k} \sum_{q=0}^{j+\ell} \frac{(-i)^j (-\alpha)^{n-i-j}}{i! j! (n-i-j)!} \frac{(i)^\ell (-\beta^*)^{n-k-\ell}}{k! \ell! (n-k-\ell)!} \right. \\
&\quad \left. \times \gamma_{(i+k), p} \gamma_{(j+\ell), q} (\alpha^* + \beta)^p (-i(\alpha^* - \beta)) \right|^q \Big|^2
\end{aligned} \tag{26}$$

where

$$\gamma_{r,j} := \begin{cases} \Gamma\left(\frac{1}{2} + \frac{r}{2}\right) \frac{(r/2)!}{2^{j/2} (1/2)_{j/2}}, & r, j \text{ even} \\ \Gamma\left(\frac{3}{2} + \frac{r-1}{2}\right) \frac{((r-1)/2)!}{2^{j-1} (3/2)_{(j-1)/2}}, & r, j \text{ odd} \\ 0, & \text{otherwise} \end{cases} \tag{27}$$

are constants, which depend on the integer values of $r \geq 0$ and $j \leq r$, and $(x)_j$ is the Pochhammer symbol. In appendix E 2, we list the explicit form of this kernel for the first 9 Fock states.

From Eq. (26), it is clear that the displacement kernel is the product of a Gaussian and a polynomial of degree $4n$ in both α and β , because

$$\begin{aligned}
2(i+k+j+\ell+(n-i-j)) &= 2(n+k+\ell) \\
&\xrightarrow[\ell]{\max} 2(n+k+(n-k)) = 4n \\
2(i+k+j+\ell+(n-k-\ell)) &= 2(n+i+j) \\
&\xrightarrow[j]{\max} 2(n+i+(n-i)) = 4n
\end{aligned}$$

Using this closed form expression we are also able to show that the kernel is translation (shift) and rotation invariant (see appendices E 3 and E 4). From these properties, we find that (see appendix E 5)

$$k(\boldsymbol{\alpha}, \boldsymbol{\beta}) = k(|\boldsymbol{\alpha} - \boldsymbol{\beta}|), \tag{28}$$

and so it is a radial kernel. This combined with the fact that the Fourier transform of this kernel is also the product of a Gaussian and a polynomial of degree $4n$, which has support over the entire Fourier domain, except at a finite number of points (see appendix E 6), means that the displaced Fock state kernel is a characteristic kernel [44].

In order to generate some intuition as to how such a kernel will behave, in figure 2 we plot the displaced Fock state kernel function, $k(|\boldsymbol{\alpha} - \boldsymbol{\beta}|)$, for test data chosen from a uniform distribution of $|\boldsymbol{\alpha} - \boldsymbol{\beta}|$ from 0 to 6, for various values of the stellar rank, n . We see in the figure that as the value of n increases, so does the number of zeros in the kernel function, as expected. Additionally, as the stellar rank increases, the kernel's ability to distinguish between large distances in the original data space, $|\boldsymbol{\alpha} - \boldsymbol{\beta}|$, improves. For example, the $n = 2$ kernel function will evaluate as zero for any distance $|\boldsymbol{\alpha} - \boldsymbol{\beta}|$ greater than 4, whereas the $n = 8$ kernel will have non-zero values up to a distance of 6. We can also see that for kernels of finite stellar rank, due to multiplication by the Gaussian factor $e^{-|\boldsymbol{\alpha} - \boldsymbol{\beta}|^2}$, there will be a threshold value beyond which all kernel evaluations will be exponentially close to zero. Additionally, it appears that as stellar rank increases, the amplitude of the non-zero kernel values diminishes, which hints that kernels of high stellar rank will have values that become increasingly concentrated around zero. This is further supported by the fact that the Fock state kernels integrate to a fixed value of π with respect to $|\boldsymbol{\alpha} - \boldsymbol{\beta}|^2$ (appendix E 7). We would expect, therefore, that CV kernels of high stellar rank will be increasingly vulnerable to noise. Recall that kernel values are always statistically approximated by repeated measurement, so as kernel values become smaller, they will require more measurements to remain distinguishable, and consequently will be increasingly vulnerable to shot noise.

This observation has some of the flavour of exponential concentration and recent work has proposed bandwidth tuning as a possible mitigation technique [25]. Let us therefore consider the consequences of implementing a bandwidth c on the encoded data by taking

$$\boldsymbol{\alpha} \rightarrow c\boldsymbol{\alpha}, \tag{29}$$

where $c \in (0, 1]$ is a real hyperparameter. Physically, this corresponds to a reduction in the value of the displacement of the Fock state, $\hat{D}(\boldsymbol{\alpha})|n\rangle \rightarrow \hat{D}(c\boldsymbol{\alpha})|n\rangle$, which results non-linear transformation of the kernel.

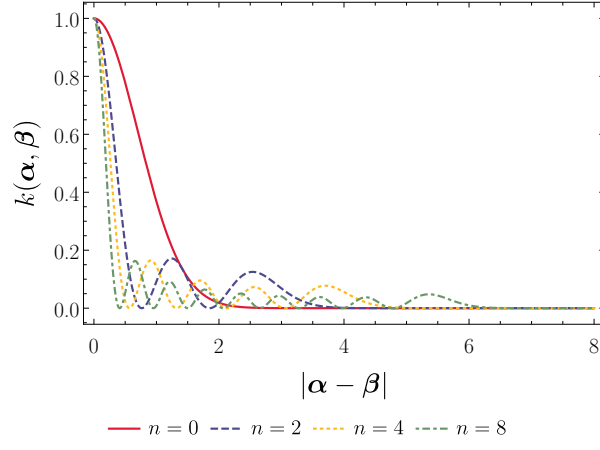


FIG. 2. The kernel function in the case of displacement encoding (Eq. (23)) as a function of $|\alpha - \beta|$, the distance in the data space, for various values of the initial Fock state, n .

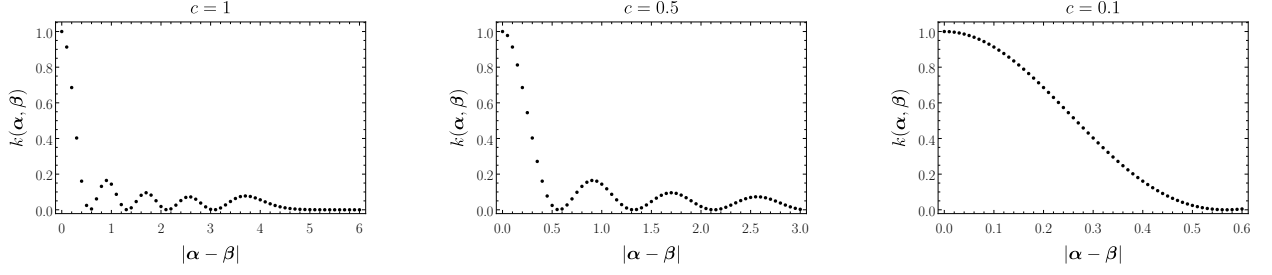


FIG. 3. The kernel function in the case of displacement encoding (Eq. (23)) with $n = 4$ for a uniform distribution of $|\alpha - \beta| \in c[0, 6]$ where c is the bandwidth hyperparameter set to (left) $c = 1$, (centre) $c = 0.5$, and (right) $c = 0.1$.

In figure 3, we explore the effect of the bandwidth c on the value of the displaced Fock state kernel function. We take some test data, which we choose to be a uniform distribution of $|\alpha - \beta|$ from 0 to 6, and apply a bandwidth so that

$$|\alpha - \beta| \rightarrow |c\alpha - c\beta| = c|\alpha - \beta|. \quad (30)$$

We find that for this particular choice of test data, a bandwidth of $c = 0.5$ (centre figure), moves all of the data away from the tail of the function (where values are exponentially close to zero). For example, all data separated in the original space by values > 5 but < 6 have kernel values of near zero for $c = 1$ (left figure) but for a bandwidth of $c = 0.5$, we can see these data points can now be discriminated. Unfortunately, it is also the case that data points that were easily distinguishable for $c = 1$, such as the two points closest to the y axis, are less distinguishable following bandwidth tuning to $c = 0.5$. Furthermore, we also see that this bandwidth reduces the *effective* stellar rank of the kernel function, since there are now only $n = 4$ maxima, rather than $n = 5$ over the range of the test data (although we note that the actual stellar rank of the kernel function does not change, since it is still defined for all $|\alpha - \beta| \in [0, \infty)$). The right figure corresponds to a bandwidth of $c = 0.1$. In this case, the kernel function is effectively a Gaussian, and consequently classically simulable. In conclusion, it is reasonable to expect that the hyperparameter, c will need to be carefully chosen for each problem. At the very least $\max(|\alpha - \beta|)$ should lie within the last maxima of the kernel function in order maximize distinguishability of each pair of data points, but without reducing the effective stellar rank so much that it becomes classically simulable).

B. Displacement & Phase

Another Gaussian operator is the phase shift operator, $\hat{R}(\varphi)$, which acts on a holomorphic function as

$$F^*(z) \mapsto F^*(e^{i\varphi}z). \quad (31)$$

We will apply this, along with the displacement operator to a Fock state $|n\rangle$ to encode a third number, $0 \leq \varphi < 2\pi$, so that now

$$\boldsymbol{\alpha} = (\alpha_1, \alpha_2, \varphi)^\top \in \mathcal{X} \subset \mathbb{R}^2 \times [0, 2\pi). \quad (32)$$

If the phase operator acts on the Fock state before the displacement operator,

$$\begin{aligned} \hat{D}(\alpha)\hat{R}(\varphi)|n\rangle &\rightarrow \hat{D}(\alpha)\frac{(e^{i\varphi}z)^n}{\sqrt{n!}} = e^{\alpha z - |\alpha|^2/2} \frac{(e^{i\varphi}(z - \alpha^*))^n}{\sqrt{n!}} \\ &= e^{in\varphi} e^{\alpha z - |\alpha|^2/2} \frac{(z - \alpha^*)^n}{\sqrt{n!}} \\ &= e^{in\varphi} \hat{D}(\alpha)|n\rangle \end{aligned} \quad (33)$$

the resulting holomorphic function differs from the displaced Fock state encoding Eq. (23) only by a phase. Therefore, a kernel with this encoding will reduce to the displaced Fock state kernel, i.e.

$$\left| \langle n | \hat{R}^\dagger(\varphi) \hat{D}^\dagger(\alpha) \hat{D}(\beta) \hat{R}(\vartheta) | n \rangle \right|^2 = \left| \langle n | \hat{D}^\dagger(\alpha) \hat{D}(\beta) | n \rangle \right|^2. \quad (34)$$

Alternatively, we can apply displacement operator to a Fock state $|n\rangle$, followed by a phase shift operator

$$\begin{aligned} \hat{R}(\varphi)\hat{D}(\alpha)|n\rangle &\rightarrow \hat{R}(\varphi) e^{\alpha z - |\alpha|^2/2} \frac{(z - \alpha^*)^n}{\sqrt{n!}} \\ &= \exp\left(e^{i\varphi}\alpha z - \frac{|\alpha|^2}{2}\right) \frac{(e^{i\varphi}z - \alpha^*)^n}{\sqrt{n!}}. \end{aligned} \quad (35)$$

as the encoding of $\boldsymbol{\alpha}$.

With this encoding, the kernel is easy to calculate by noting that taking $\alpha \rightarrow e^{i\varphi}\alpha$ in Eq. (33) results in Eq. (35), and so applying this transformation to Eq. (26), results in the phase-displacement kernel:

$$\begin{aligned} k_{RD}(\boldsymbol{\alpha}, \boldsymbol{\beta}) &= \left| \langle F_{\alpha, \varphi}^*(z) | F_{\beta, \vartheta}^*(z) \rangle \right|^2 \\ &= \left(\frac{n!}{\pi} \right)^2 e^{-|\alpha - \beta|^2} \left| \sum_{i=0}^n \sum_{j=0}^{n-i} \sum_{k=0}^n \sum_{\ell=0}^{n-k} \sum_{p=0}^{n-k-\ell} \sum_{q=0}^{j+\ell} \frac{(-i)^j e^{i(n-i-j)\varphi} (-\alpha)^{n-i-j}}{i!j!(n-i-j)!} \right. \\ &\quad \times \frac{(i)^\ell e^{-i(n-p-q)\vartheta} (-\beta^*)^{n-k-\ell}}{k!\ell!(n-k-\ell)!} \gamma_{(i+k), p} \gamma_{(j+\ell), q} \\ &\quad \left. \times (e^{-i\varphi}\alpha^* + e^{i\vartheta}\beta)^p (-i(e^{-i\varphi}\alpha^* - e^{i\vartheta}\beta))^q \right|^2 \end{aligned} \quad (36)$$

where $\gamma_{r,j}$ is defined in Eq. (27).

Unlike the displaced Fock state kernel, the phase-displacement kernel is not, in general, translation invariant. Consider the $n = 1$, where

$$\begin{aligned} \langle F_{\alpha, \varphi}^*(z) | F_{\beta, \vartheta}^*(z) \rangle &= \exp\left(-\frac{|\alpha|^2 + |\beta|^2}{2}\right) \exp\left(e^{i(\vartheta - \varphi)}\alpha^*\beta\right) \exp(i(\vartheta - \varphi)) \\ &\quad \times \left[1 - |\alpha|^2 - |\beta|^2 + 2\operatorname{Re}\left(e^{i(\vartheta - \varphi)}\alpha^*\beta\right)\right] \end{aligned} \quad (37)$$

and apply a translation of $\mathbf{h} = (h_1, h_2, \eta)^\top$, where $h_1, h_2 \in \mathbb{R}$ and $\eta \in [0, 2\pi)$. Additionally, define $h = h_1 + ih_2$, so the shifted kernel is:

$$k_{RD}(\boldsymbol{\alpha} + \mathbf{h}, \boldsymbol{\beta} + \mathbf{h}) = \left| \langle F_{\alpha+h, \varphi+\eta}^*(z) | F_{\beta+h, \vartheta+\eta}^*(z) \rangle \right|^2 \quad (38)$$

where

$$\begin{aligned}
& \langle F_{\alpha+h, \varphi+\eta}^*(z) | F_{\beta+h, \vartheta+\eta}^*(z) \rangle \\
&= \exp \left(-\frac{|\alpha|^2 + |\beta|^2}{2} \right) \exp \left(e^{i(\vartheta-\varphi)} \alpha^* \beta \right) \exp \left(i \operatorname{Im} (h(\alpha^* - \beta^*)) \right) \\
&\quad \times \exp \left((e^{i(\vartheta-\varphi)} - 1) (|h|^2 + h\alpha^* + h^*\beta) \right) \exp (i(\vartheta - \varphi)) \\
&\quad \times \left[1 - |\alpha|^2 - |\beta|^2 + 2 \operatorname{Re} \left(e^{i(\vartheta-\varphi)} \alpha^* \beta \right) + 2 \operatorname{Re} \left((e^{i(\vartheta-\varphi)} - 1) (h\alpha^* + h^*\beta) \right) \right. \\
&\quad \left. - 4 |h|^2 \sin^2 \left(\frac{\vartheta - \varphi}{2} \right) \right].
\end{aligned} \tag{39}$$

This clearly depends on \mathbf{h} by more than a phase, so the kernel will also be dependent on \mathbf{h} .

Since this kernel is not shift invariant

$$k_{RD}(\alpha, \beta) \neq k_{RD}(\alpha - \beta), \tag{40}$$

it is a function of all five encoded parameters: $\alpha_1, \alpha_2, \beta_1, \beta_2$ and the phase difference $(\vartheta - \varphi)$. However, on closer examination, we find that most of the complexity of the resulting kernel can be captured by the phase shift. In figure 4 we explore this additional complexity, by plotting the kernel function as function of two encoded variables, α_1 and β_1 for various values of $(\vartheta - \varphi)$ and a fixed value of α_2 and β_2 . In all four figures, we find similar behaviour of the kernel; there is an overall elliptical profile with six maxima and five minima, corresponding to the stellar rank of $n = 5$. Additionally, the Gaussian part of the kernel exponentially suppresses kernel values that are sufficiently far from the maximum. The overall eccentricity of the envelope depends on the phase difference. We find similar behaviour for the kernel function plotted as a function of α_2 and β_2 as well as plotted as a function of α_1 and β_2 .

Next, we consider how bandwidth modifies the kernel by rescaling the encoded data $(\alpha_1, \alpha_2) \rightarrow c(\alpha_1, \alpha_2)$ and $(\beta_1, \beta_2) \rightarrow c(\beta_1, \beta_2)$ with $c \in (0, 1]$. Physically, this corresponds to a reduction in the size of the displacement of the initial Fock state. This type of bandwidth is shown in figure 5, where the kernel function is plotted as a function of the phase difference, $\vartheta - \varphi$ for fixed values of $c\alpha_1, c\alpha_2, c\beta_1$ and $c\beta_2$ and various values of the hyperparameter c . We find that, when $c = 1$, as shown in the left column, the value of the kernel function is exponentially suppressed for values of $\vartheta - \varphi$ far from π . As c is decreased (as shown in the centre column) the kernel function is, on average, larger than the $c = 1$ case for all values of $\vartheta - \varphi$; however, there is a loss of effective stellar rank of the kernel function. Again, if the value of c is too small (as shown in the right column), the kernel function is nearly a Gaussian, indicating loss of any quantum advantage. This once again indicates the existence of a target problem specific optimal value of c . While bandwidth tuning appears to mean one must choose between minimising kernel concentration to enhance learnability and maintaining effective stellar rank and hence quantum advantage, it is clear that different values will have distinct implications for each specific encoding and also each particular problem.

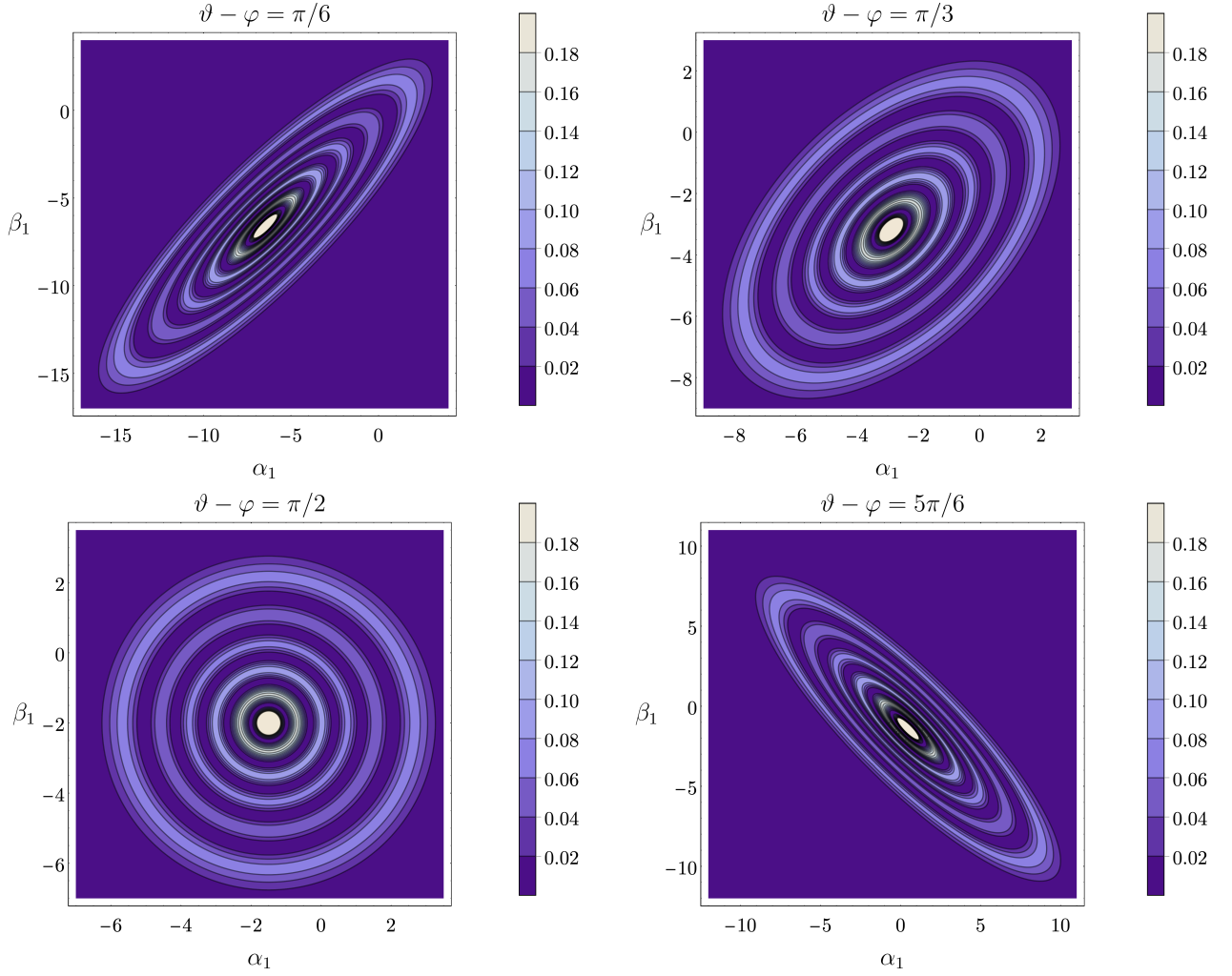


FIG. 4. Here we depict two dimensional slices of the five dimensional kernel function in the case of displacement and phase shift encoding (Eq. (33)) with $n = 5$ as a function of the encoded real parameters α_1 and β_1 for the various values of the encoded: (top left) $\vartheta - \varphi = \pi/6$, (top right) $\vartheta - \varphi = \pi/3$, (bottom left) $\vartheta - \varphi = \pi/2$ and (bottom right) $\vartheta - \varphi = 5\pi/6$. The remaining real parameters are set to $\alpha_2 = -2$ and $\beta_2 = 1.5$.

C. General Kernel (Multi-Mode)

We have provided some intuition for the behaviour of two simple CV kernel building blocks. It is clear, however, that it is unlikely that kernels that can only encode data of two or three dimensions will have much utility. We therefore now consider combining such kernels via multi-mode bosonic states to enable the encoding of high dimensional data. A first challenge is to understand if we can still write such kernels in closed form.

A general m -mode bosonic state of total stellar rank n can be represented by the holomorphic function

$$F^*(\mathbf{z}) = G(\mathbf{z})P(\mathbf{z}) \quad (41)$$

where $\mathbf{z} = (z_1, z_2, \dots, z_m)^\top$, $G(\mathbf{z})$ is a Gaussian and $P(\mathbf{z})$ is a polynomial[34].

In general,

$$\begin{aligned} G(\mathbf{z}) &= \exp\left(-\frac{1}{2}\mathbf{z}^\top A \mathbf{z} + B^\top \mathbf{z} + C\right) \\ P(\mathbf{z}) &= \sum_{\substack{i_1, i_2, \dots, i_m \geq 0 \\ i_1 + i_2 + \dots + i_m = n}} \beta_{\mathbf{i}} z_1^{i_1} z_2^{i_2} \dots z_m^{i_m} \end{aligned} \quad (42)$$

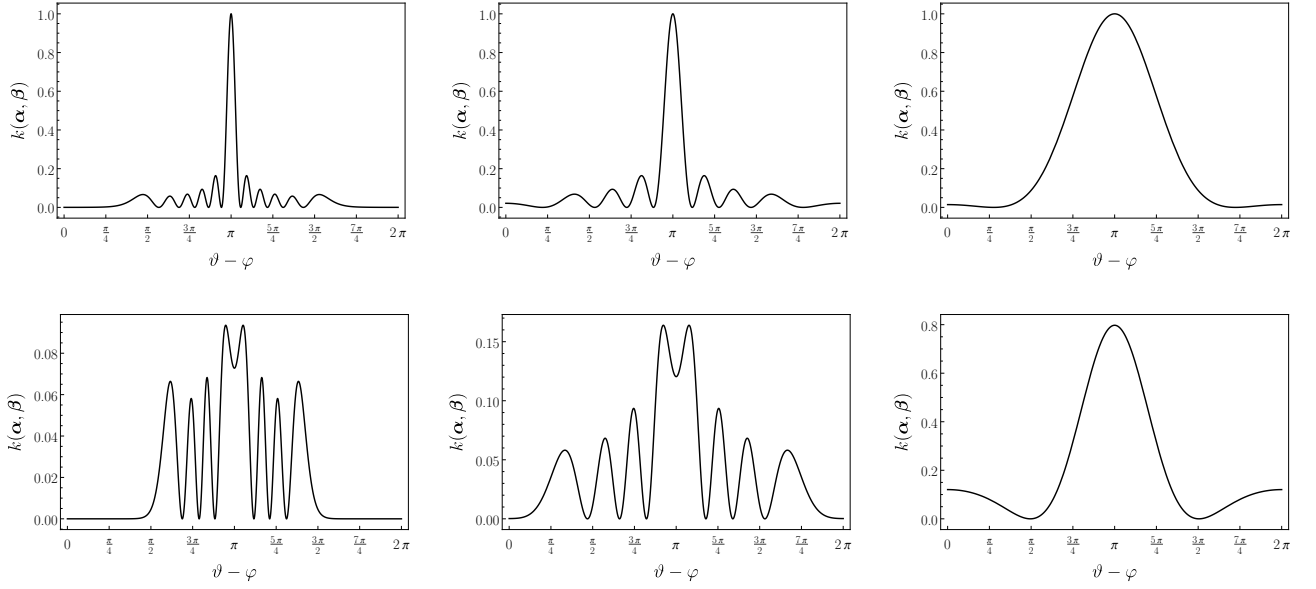


FIG. 5. Here we depict one dimensional slices of the five dimensional kernel function in the case of displacement and phase shift encoding (Eq. (33)) with $n = 5$ as a function of the encoded angles $\vartheta - \varphi$. The encoded real parameters are (*top row*) $\alpha_1 = \alpha_2 = c \times 2$ and $\beta_1 = \beta_2 = c \times (-2)$ and, (*bottom row*) $\alpha_1 = -\alpha_2 = c \times 2$ and $\beta_1 = -\beta_2 = c \times (-3)$ where c is the bandwidth hyperparameter. The bandwidth is set to (*left column*) $c = 1$, (*centre column*) $c = 0.5$, and (*right column*) $c = 0.1$.

where $A \in \mathbb{C}^m \times \mathbb{C}^m$ with components $A_{i,j}$ and $\text{Re}(A_{jj}) > 0$, $B \in \mathbb{C}^m$ with components B_j , $\mathbf{i} := (i_1, i_2, \dots, i_m)$, and $C, \beta_{\mathbf{i}} \in \mathbb{C}$.

Given some encoding of data $\mathbf{x}_1, \mathbf{x}_2 \in \mathcal{X}$ into such a state, the quantum kernel is

$$k(\mathbf{x}_1, \mathbf{x}_2) = |\langle F_{\mathbf{x}_1}^* | F_{\mathbf{x}_2}^* \rangle|^2 \quad (43)$$

where

$$\begin{aligned} \langle F_{\mathbf{x}_1}^* | F_{\mathbf{x}_2}^* \rangle &= \frac{1}{\pi^m} \int_{\mathbf{z} \in \mathbb{C}^m} d^{2m} z \, e^{-|\mathbf{z}|^2} F_{\mathbf{x}_1}(\mathbf{z})^* F_{\mathbf{x}_2}(\mathbf{z}) \\ &= \frac{1}{\pi^m} \int_{\mathbf{z} \in \mathbb{C}^m} d^{2m} z \, e^{-|\mathbf{z}|^2} \exp \left(-\frac{1}{2} \mathbf{z}^\dagger A^{(1)*} \mathbf{z}^* + B^{(1)\dagger} \mathbf{z}^* + C^{(1)*} \right) \\ &\quad \times \left(\sum_{i_1+i_2+\dots+i_m=n} \beta_{\mathbf{i}}^{(1)*} (z_1^*)^{i_1} (z_2^*)^{i_2} \dots (z_n^*)^{i_n} \right) \\ &\quad \times \exp \left(-\frac{1}{2} \mathbf{z}^\dagger A^{(2)} \mathbf{z} + B^{(2)\dagger} \mathbf{z} + C^{(2)} \right) \left(\sum_{j_1+j_2+\dots+j_n=n} \beta_{\mathbf{j}}^{(2)} z_1^{j_1} z_2^{j_2} \dots z_n^{j_n} \right) \end{aligned} \quad (44)$$

and the superscripts keep track of the encoded data.

Calculating this inner product (see appendix D 1) requires the evaluation of $2m$ integrals, each of the form

$$\begin{aligned} I_r(a, b) &:= \int_{-\infty}^{\infty} dx \, \exp(-ax^2 + bx) x^r \\ &= a^{-(r+1)/2} \exp\left(\frac{b^2}{4a}\right) \sum_{j=0}^r \gamma_{r,j} \left(\frac{b}{\sqrt{a}}\right)^j \end{aligned} \quad (45)$$

where the $\gamma_{r,j}$'s are defined in Eq. (27). This can be done algorithmically, (see appendix F), and we are able to obtain

a closed form expression for the general m -mode kernel

$$\begin{aligned} \langle F_{x_1}^* | F_{x_2}^* \rangle &= \frac{1}{\pi^m} \exp \left(C^{(1)*} + C^{(2)} + \sum_{j=1}^{2m} \frac{b_{j-1,j}^2}{4a_{j-1,j}} \right) \sum_{i_1+\dots+i_m=n} \sum_{j_1+\dots+j_m=n} \beta_i^{(1)*} \beta_j^{(2)} \\ &\times \sum_{\mathbf{p}=\mathbf{0}}^{\mathbf{i}} \sum_{\mathbf{q}=\mathbf{0}}^{\mathbf{j}} \prod_{\ell=1}^{2m-1} \left(\sum_{s_\ell=0}^{r_{\ell-1,\ell}} \frac{\gamma_{r_{\ell-1,\ell},s_\ell}}{a_{\ell-1,\ell}^{(r_{\ell-1,\ell}+s_\ell+1)/2}} \sum_{t_\ell=0}^{s_\ell} \frac{s_\ell!}{(s_\ell-t_\ell)!} b_{\ell-1,\ell}^{s_\ell-t_\ell} \right. \\ &\times \left. \sum_{u_{\ell,\ell+1}+\dots+u_{\ell,2m}=t_\ell} g_{\ell,\ell+1} \right) \left(\sum_{s_{2m}=0}^{r_{2m-1,2m}} \frac{\gamma_{r_{2m-1,2m},s_{2m}}}{a_{2m-1,2m}^{(r_{2m-1,2m}+s_{2m}+1)/2}} b_{2m-1,2m}^{s_{2m}} \right) \end{aligned} \quad (46)$$

where a , b , d , g , and r are defined recursively as

$$\begin{aligned} a_{i,j} &:= a_{i-1,j} - \frac{d_{i-1,i,j}^2}{4a_{i-1,j}} \\ b_{i,j} &:= b_{i-1,j} + \frac{b_{i-1,i}d_{i-1,i,j}}{2a_{i-1,i}} \\ d_{i,j,k} &:= d_{i-1,j,k} + \frac{d_{i-1,i,j}d_{i-1,i,k}}{2a_{i-1,i}} \end{aligned} \quad (47)$$

which depend, in part, on the initial encoding of x_1 and x_2 and

$$\begin{aligned} g_{i,k} &:= \frac{g_{i-1,k}d_{i-1,i,k}^{u_{i,k}}}{u_{i,k}!} \\ r_{i,k} &:= r_{i-1,k} + u_{i,k}. \end{aligned} \quad (48)$$

The initial values of these parameters are defined in appendix F.

We note that any CV encoding will always have a kernel of the form of Eq.(46), and can be expressed as a product of a Gaussian and a polynomial of degree $4n$. Hence, according to [35], the strong classical simulability of the general CV quantum kernel (equation 46) scales exponentially on the order of $\mathcal{O}(2^{4n})$. Furthermore, from equation 46 it appears that classically simulating the kernel also scales exponentially in m , the mode of the encoding, given that $m \leq n$. The scaling with m comes from the general form within the product of sums,

$$\prod_{l=1}^{2m-1} (\dots), \quad (49)$$

representing a deeply nested sum of depth $2m-1$. Each of the sums within this product are dependent on the index of prior sums and the total length of each sum also increases as a function of m . It can be easily seen that the computational complexity of m nested sums each of length $\geq l$ scales as $\mathcal{O}(l^m)$. As such, we see that our general kernel's classical simulability scales as at least $\mathcal{O}(l^m)$ for some $l > 1$ which we can fix.

This is a useful property as in practice the easiest way of increasing the stellar rank of a CV quantum state is to increase the number of modes rather than directly increasing the stellar rank of a single mode.

D. Qudit Kernels

Thus far we have only examined the CV case and it is interesting to ask if any of our results are applicable in the more familiar discrete qubit/qudit case. In fact, qudits of dimension d can also be represented as complex polynomials in the SB space as [34]

$$|\psi\rangle = \sum_{j=0}^{d-1} \alpha_j |j\rangle \rightarrow F_\psi^*(z) = \sum_{j=0}^{d-1} n_{d,j} \alpha_j z^j \quad (50)$$

where $n_{d,j} \in \mathbb{C}$ is a normalization factor, which only depends on d and j and ensures that

$$\langle F_\psi^*(z) | F_\psi^*(z) \rangle_{SB} = \sum_{j=0}^{d-1} |\alpha_j|^2 = 1. \quad (51)$$

We note that a tensor product of m qudits, each of dimension d , can always be written as a single qudit of dimension $m \times d$, so we will only consider the single mode case.

As with the CV kernels, we consider the qudit kernel to be

$$k(x_1, x_2) = |\langle \psi(x_1) | \psi(x_2) \rangle|^2 \quad (52)$$

where the data $x_1, x_2 \in \mathcal{C}$ are encoded into the states $|\psi(x_1)\rangle$ and $|\psi(x_2)\rangle$ respectively. In the case of mixed states, where the data is encoded into a density matrix $\hat{\rho}(x) \in \mathbb{C}^d \otimes \mathbb{C}^d$, we will consider the vectorisation, which stacks the columns of the matrix to form a single vector $|\rho(x)\rangle \in \mathbb{C}^{2d}$ [1]. The vectorised state can then be represented as Eq. (50).

With the encoded qudits represented as polynomials in the SB space, we can calculate the inner product as (see appendix G):

$$\begin{aligned} \langle \psi(x_1) | \psi(x_2) \rangle &\rightarrow \langle F_1^*(z) | F_2^*(z) \rangle = \frac{1}{\pi} \int_{z \in \mathbb{C}} d^2z e^{-z^2} \left(\sum_{i=0}^{d-1} n_{d,i}^* \alpha_i^{(1)*} (z^*)^i \right) \left(\sum_{j=0}^{d-1} n_{d,j} \alpha_j^{(2)} z^j \right) \\ &= \sum_{i=0}^{d-1} \sum_{j=0}^{d-1} \frac{1 + (-1)^{i+j}}{2} \frac{1}{2^{(i+j)}} n_{d,i}^* n_{d,j} \alpha_i^{(1)*} \alpha_j^{(2)} \sum_{p=0}^i \sum_{q=0}^j (-1)^q \binom{i}{p} \binom{j}{q} \\ &\quad \times \cos\left(\frac{\pi(p+q)}{2}\right) \frac{(p+q)!}{(p+q)/2)!} \frac{(i+j-p-q)!}{(i+j-p-q)/2)!}. \end{aligned} \quad (53)$$

The same expression can also be calculated from the general multi-mode kernel (Eq. (46), by setting $m = 1$, $n = d - 1$ and $\beta_j = n_{d,j} \alpha_j$ (see appendix G 1), showing that *all* quantum kernels that can be written as Eq. (3) can be written as the product of a Gaussian and a polynomial.

VI. CONCLUSIONS & FUTURE WORK

In this paper we use the holomorphic representation of continuous variable quantum states to mathematically describe how one might encode data for CV quantum kernel machine learning. In doing so, we are able to identify that all quantum kernels can be expressed analytically as products of Gaussian and polynomial terms. The measure of stellar rank, a quantity that is easy to characterise for practical bosonic implementations, neatly captures the classical hardness of simulating these kernels, which scales as $\mathcal{O}(2^{4n})$. Furthermore, by analysing several simple CV kernels we are able to develop intuition for how such kernels will behave as we increase their “quantumness” as measured by stellar rank. We see that it is likely that one will encounter problems analogous to exponential concentration, and while bandwidth tuning may mitigate this to some extent, this will trade-off with maintaining effective stellar rank and robustness to shot noise. We have also shown that it is possible to construct CV quantum kernels that embody both translational and rotational invariance - such kernels may have application to problem sets with a similar underlying structure.

We have further shown that while multi-mode CV quantum kernels are more complex, they can nonetheless still always be expressed as a product of Gaussian and polynomial terms and their classical simulability will still scale exponentially with stellar rank. While we haven’t simulated such kernels here, we would expect similar behaviour in terms of kernel concentration beyond a threshold value due to the Gaussian term, and also exponential concentration as stellar rank increases. It will be important in future work to quantitatively characterise the bandwidth generated trade-offs for particular target problems and specific physical implementations, and analyse the effects of various appropriate noise models.

ACKNOWLEDGEMENTS

This work has been supported by the Australian Research Council (ARC) by Centre of Excellence for Engineered Quantum Systems (EQUS, CE170100009). We wish to thank Aleesha Isaacs, Carolyn Wood, Gerard Milburn and Andrew White for useful discussions.

[1] M. Schuld, Supervised quantum machine learning models are kernel methods (2021), [arXiv:2101.11020](https://arxiv.org/abs/2101.11020) [quant-ph].

- [2] M. Schuld and N. Killoran, Quantum machine learning in feature hilbert spaces, *Phys. Rev. Lett.* **122**, 040504 (2019).
- [3] M. P. SCHULD, *Supervised learning with Quantum Computers* (SPRINGER, 2019).
- [4] P. Wittek, *Quantum Machine Learning: What quantum computing means to data mining* (Academic Press is an imprint of Elsevier, 2016).
- [5] I. Goodfellow, Y. Bengio, and A. Courville, *Deep Learning* (MIT Press, 2016).
- [6] Y.-H. H. Tsai, S. Bai, M. Yamada, L.-P. Morency, and R. Salakhutdinov, Transformer dissection: An unified understanding for transformer’s attention via the lens of kernel, in *Proceedings of the 2019 Conference on Empirical Methods in Natural Language Processing and the 9th International Joint Conference on Natural Language Processing (EMNLP-IJCNLP)*, edited by K. Inui, J. Jiang, V. Ng, and X. Wan (Association for Computational Linguistics, Hong Kong, China, 2019) pp. 4344–4353.
- [7] M. Bińkowski, D. J. Sutherland, M. Arbel, and A. Gretton, Demystifying MMD GANs, in *International Conference on Learning Representations* (2018).
- [8] J. Mitrovic, D. Sejdinovic, and Y. W. Teh, Causal inference via kernel deviance measures, *Advances in neural information processing systems* **31** (2018).
- [9] S. An, W. Liu, and S. Venkatesh, Face recognition using kernel ridge regression, in *2007 IEEE Conference on Computer Vision and Pattern Recognition* (2007) pp. 1–7.
- [10] W. Liu, I. Park, and J. C. Principe, An information theoretic approach of designing sparse kernel adaptive filters, *IEEE Transactions on Neural Networks* **20**, 1950 (2009).
- [11] S. Akaho, A kernel method for canonical correlation analysis (2007), [arXiv:cs/0609071 \[cs.LG\]](https://arxiv.org/abs/cs/0609071).
- [12] M. Belkin, S. Ma, and S. Mandal, To understand deep learning we need to understand kernel learning, in *Proceedings of the 35th International Conference on Machine Learning*, Proceedings of Machine Learning Research, Vol. 80, edited by J. Dy and A. Krause (PMLR, 2018) pp. 541–549.
- [13] Y. Cho and L. Saul, Kernel methods for deep learning, in *Advances in Neural Information Processing Systems*, Vol. 22, edited by Y. Bengio, D. Schuurmans, J. Lafferty, C. Williams, and A. Culotta (Curran Associates, Inc., 2009).
- [14] T. Hubregtsen, D. Wierichs, E. Gil-Fuster, P.-J. H. S. Derks, P. K. Faehrmann, and J. J. Meyer, Training quantum embedding kernels on near-term quantum computers, *Physical Review A* **106**, 10.1103/physreva.106.042431 (2022).
- [15] C. Gyurik, v. Dyon Vreumingen, and V. Dunjko, Structural risk minimization for quantum linear classifiers, *Quantum* **7**, 893 (2023).
- [16] S. Jerbi, L. J. Fiderer, H. P. Nautrup, J. M. Kübler, H. J. Briegel, and V. Dunjko, Quantum machine learning beyond kernel methods, *Nature Communications* **14**, 10.1038/s41467-023-36159-y (2023).
- [17] Y. Liu, S. Arunachalam, and K. Temme, A rigorous and robust quantum speed-up in supervised machine learning, *Nature Physics* **17**, 1013 (2021).
- [18] J. R. Glick, T. P. Gujarati, A. D. Corcoles, Y. Kim, A. Kandala, J. M. Gambetta, and K. Temme, Covariant quantum kernels for data with group structure (2022), [arXiv:2105.03406 \[quant-ph\]](https://arxiv.org/abs/2105.03406).
- [19] V. Havlíček, A. D. Córcoles, K. Temme, A. W. Harrow, A. Kandala, J. M. Chow, and J. M. Gambetta, Supervised learning with quantum-enhanced feature spaces, *Nature* **567**, 209–212 (2019).
- [20] H.-Y. Huang, M. Broughton, J. Cotler, S. Chen, J. Li, M. Mohseni, H. Neven, R. Babbush, R. Kueng, J. Preskill, and J. R. McClean, Quantum advantage in learning from experiments, *Science* **376**, 1182 (2022), <https://www.science.org/doi/pdf/10.1126/science.abn7293>.
- [21] J. R. McClean, S. Boixo, V. N. Smelyanskiy, R. Babbush, and H. Neven, Barren plateaus in quantum neural network training landscapes, *Nature Communications* **9**, 10.1038/s41467-018-07090-4 (2018).
- [22] S. Thanasilp, S. Wang, M. Cerezo, and Z. Holmes, Exponential concentration and untrainability in quantum kernel methods (2022), [arXiv:2208.11060 \[quant-ph\]](https://arxiv.org/abs/2208.11060).
- [23] J. M. Kübler, S. Buchholz, and B. Scholkopf, The inductive bias of quantum kernels, in *Neural Information Processing Systems* (2021).
- [24] H.-Y. Huang, M. Broughton, M. Mohseni, R. Babbush, S. Boixo, H. Neven, and J. R. McClean, Power of data in quantum machine learning, *Nature Communications* **12**, 10.1038/s41467-021-22539-9 (2021).
- [25] A. Canatar, E. Peters, C. Pehlevan, S. M. Wild, and R. Shaydulin, Bandwidth enables generalization in quantum kernel models, *Transactions on Machine Learning Research* (2023).
- [26] A. Canatar, *Statistical Mechanics of Generalization in Kernel Regression and Wide Neural Networks*, Doctoral dissertation, Harvard University Graduate School of Arts and Sciences (2022).
- [27] B. Schölkopf and A. J. Smola, *Learning with kernels: Support vector machines, regularization, optimization and beyond* (MIT press, 2002).
- [28] L. Slattey, R. Shaydulin, S. Chakrabarti, M. Pistoia, S. Khairy, and S. M. Wild, Numerical evidence against advantage with quantum fidelity kernels on classical data, *Physical Review A* **107**, 10.1103/physreva.107.062417 (2023).
- [29] M. Ragone, P. Braccia, Q. T. Nguyen, L. Schatzki, P. J. Coles, F. Sauvage, M. Larocca, and M. Cerezo, Representation theory for geometric quantum machine learning (2023), [arXiv:2210.07980 \[quant-ph\]](https://arxiv.org/abs/2210.07980).
- [30] R. Ghobadi, Nonclassical kernels in continuous-variable systems, *Phys. Rev. A* **104**, 052403 (2021).
- [31] P. Tiwari, S. Dehdashti, A. K. Obeid, P. Marttinen, and P. Bruza, Kernel method based on non-linear coherent states in quantum feature space, *Journal of Physics A: Mathematical and Theoretical* **55**, 355301 (2022).
- [32] J. Liu, C. Zhong, M. Otten, A. Chandra, C. L. Cortes, C. Ti, S. K. Gray, and X. Han, Quantum kerr learning, *Machine Learning: Science and Technology* **4**, 025003 (2023).
- [33] C. Bowie, S. Shrapnel, and M. J. Kewming, Quantum kernel evaluation via hong–ou–mandel interference, *Quantum Science and Technology* **9**, 015001 (2023).

- [34] U. Chabaud and S. Mehraban, Holomorphic representation of quantum computations, [Quantum](#) **6**, 831 (2022).
- [35] U. Chabaud and M. Walschaers, Resources for bosonic quantum computational advantage, *Physical Review Letters* **130**, 10.1103/physrevlett.130.090602 (2023).
- [36] T. Hofmann, B. Schölkopf, and A. J. Smola, Kernel methods in machine learning, *The Annals of Statistics* **36**, 10.1214/0090536070000000677 (2008).
- [37] B. Schölkopf, R. Herbrich, and A. J. Smola, A generalized representer theorem, [Lecture Notes in Computer Science](#) , 416–426 (2001).
- [38] B. K. Sriperumbudur, K. Fukumizu, and G. R. Lanckriet, Universality, characteristic kernels and rkhs embedding of measures, [Journal of Machine Learning Research](#) **12**, 2389 (2011).
- [39] J. Shawe-Taylor and N. Cristianini, [Kernel Methods for Pattern Analysis](#) (Cambridge University Press, 2004).
- [40] V. V'yugin, Vc dimension, fat-shattering dimension, rademacher averages, and their applications (2015) pp. 57–74.
- [41] O. Allerbo and R. Jörnsten, Bandwidth selection for gaussian kernel ridge regression via jacobian control (2023), [arXiv:2205.11956 \[stat.ML\]](#).
- [42] D. Gottesman, The Heisenberg representation of quantum computers, (1998).
- [43] S. D. Bartlett, B. C. Sanders, S. L. Braunstein, and K. Nemoto, Efficient classical simulation of continuous variable quantum information processes, [Phys. Rev. Lett.](#) **88**, 097904 (2002).
- [44] B. Sriperumbudur, A. Gretton, K. Fukumizu, G. Lanckriet, and B. Schölkopf, Injective hilbert space embeddings of probability measures, in *Proceedings of the 21st Annual Conference on Learning Theory*, Max-Planck-Gesellschaft (Omnipress, Madison, WI, USA, 2008) pp. 111–122.
- [45] C. Scott and K. Greenewald, Universal consistency of svms and other kernel methods (2014).
- [46] V. Bargmann, On a hilbert space of analytic functions and an associated integral transform part i, [Communications on Pure and Applied Mathematics](#) **14**, 187–214 (1961).
- [47] V. I. Paulsen and M. Raghupathi, An introduction to the theory of reproducing kernel hilbert spaces (Cambridge University Press, 2016).
- [48] DLMF, [NIST Digital Library of Mathematical Functions](#), <https://dlmf.nist.gov/>, Release 1.1.11 of 2023-09-15, f. W. J. Olver, A. B. Olde Daalhuis, D. W. Lozier, B. I. Schneider, R. F. Boisvert, C. W. Clark, B. R. Miller, B. V. Saunders, H. S. Cohl, and M. A. McClain, eds.
- [49] E. W. Weisstein, [Binomial coefficient](#), visited on 05/01/24.

Supplementary Material

Appendix A: Inner Products

Remark 1. *Inner Products of the form $\langle \cdot | \cdot \rangle : \mathcal{H} \times \mathcal{H} \rightarrow \mathbb{C}$ are positive semi-definite.*

A matrix \mathbf{M} is positive semi-definite if and only if

$$\mathbf{x}^\dagger \mathbf{M} \mathbf{x} \geq 0 \quad \forall \mathbf{x} \in \mathbb{C}^n. \quad (\text{A1})$$

We can construct our Gram Matrix, \mathbf{G} , from our defined inner product by

$$G_{i,j} = \langle \mathbf{v}_i | \mathbf{v}_j \rangle, \quad (\text{A2})$$

for $\mathbf{v}_i, \mathbf{v}_j \in \mathcal{H}$.

Hence to show the inner product is positive semi-definite, it is sufficient to show the gram matrix is positive semi-definite. We can see for any $\mathbf{x} \in \mathbb{C}^n$,

$$\mathbf{x}^\dagger \mathbf{G} \mathbf{x} = \sum_{i,j} x_i^* G_{i,j} x_j \quad (\text{A3})$$

$$= \sum_{i,j} x_i^* \langle \mathbf{v}_i | \mathbf{v}_j \rangle x_j \quad (\text{A4})$$

$$= \sum_{i,j} \langle x_i^* \mathbf{v}_i | x_j \mathbf{v}_j \rangle \quad (\text{A5})$$

$$= \left\langle \sum_i x_i^* \mathbf{v}_i \left| \sum_j x_j \mathbf{v}_j \right. \right\rangle \quad (\text{A6})$$

$$= \left\| \sum_i x_i^* \mathbf{v}_i \right\|^2 \geq 0 \quad (\text{A7})$$

Remark 2. *Note that by definition, inner products are also conjugate symmetric. That is,*

$$\langle x | y \rangle = \langle y | x \rangle^*. \quad (\text{A8})$$

Appendix B: Kernel Symmetry:

To prove symmetry of our quantum kernel, let us re-write it by expanding the absolute value square as,

$$k(\mathbf{x}_1, \mathbf{x}_2) = \langle F_{\mathbf{x}_1}^*(\mathbf{z}) | F_{\mathbf{x}_2}^*(\mathbf{z}) \rangle_{SB} \langle F_{\mathbf{x}_1}^*(\mathbf{z}) | F_{\mathbf{x}_2}^*(\mathbf{z}) \rangle_{SB}^*. \quad (\text{B1})$$

Hence if we permute our data points we have,

$$k(\mathbf{x}_2, \mathbf{x}_1) = \langle F_{\mathbf{x}_2}^*(\mathbf{z}) | F_{\mathbf{x}_1}^*(\mathbf{z}) \rangle_{SB} \langle F_{\mathbf{x}_2}^*(\mathbf{z}) | F_{\mathbf{x}_1}^*(\mathbf{z}) \rangle_{SB}^*. \quad (\text{B2})$$

Here, we can apply the conjugate symmetric property of inner products (remark 2) to yield

$$\begin{aligned} k(\mathbf{x}_2, \mathbf{x}_1) &= \langle F_{\mathbf{x}_1}^*(\mathbf{z}) | F_{\mathbf{x}_2}^*(\mathbf{z}) \rangle_{SB}^* \left(\langle F_{\mathbf{x}_1}^*(\mathbf{z}) | F_{\mathbf{x}_2}^*(\mathbf{z}) \rangle_{SB} \right)^* \\ &= \langle F_{\mathbf{x}_1}^*(\mathbf{z}) | F_{\mathbf{x}_2}^*(\mathbf{z}) \rangle_{SB} \langle F_{\mathbf{x}_1}^*(\mathbf{z}) | F_{\mathbf{x}_2}^*(\mathbf{z}) \rangle_{SB}^* \\ &= k(\mathbf{x}_1, \mathbf{x}_2). \end{aligned} \quad (\text{B3})$$

Appendix C: Segal Bargmann Space is an RKHS of the Gaussian Kernel

Our formulation of CV quantum kernels heavily utilises the Segal Bargmann space. Knowing properties about this space can allow us to further develop our kernels. Here we explicitly prove that this space contains the Gaussian kernel which is well known to be universal. We can also show that this kernel is universal. Universality of kernels is a measure of their expressibility, characterising how well the kernel can classify the data from a metric space. A universal kernel is one which can learn any function for empirical loss minimisation from equation 2. To prove such a property we can show that the RKHS is dense inside the space of continuous functions ($\mathcal{C}(\mathcal{X})$) of our data. This is equivalent to showing that the kernel, decomposed into a power series of inner products, has only positive coefficients [45].

The following proof is adapted from [46]. Let us denote our reproducing kernel as $\mathbf{e}_a \in \mathcal{H}_{SB}$ for some fixed $a \in \mathcal{C}^n$. Hence by properties of the evaluation functional we have,

$$f(a) = \langle \mathbf{e}_a | f \rangle. \quad (\text{C1})$$

By the definition of the inner product in the SB space we can rewrite this as,

$$f(a) = \int_{\mathcal{C}^m} d^{2m}z \mathbf{e}_a^*(z) f(z). \quad (\text{C2})$$

Here we can see that the reproducing kernel $\mathbf{e}_a^*(z) = \mathcal{K}(a, z)$ is the kernel function for the SB space. By definition (equation C1) we have,

$$\mathbf{e}_a(z) = \langle \mathbf{e}_z | \mathbf{e}_a \rangle, \quad (\text{C3})$$

and so we yield,

$$\mathcal{K}(a, z) = \langle \mathbf{e}_a | \mathbf{e}_z \rangle. \quad (\text{C4})$$

In terms of any complete orthonormal set, v_h we can write the evaluational functional as,

$$\mathbf{e}_a = \lim_{k \rightarrow \infty} \sum_{h=1}^k \langle v_h | \mathbf{e}_a \rangle v_h = \lim_{k \rightarrow \infty} \sum_{h=1}^k v_h^*(a) v_h. \quad (\text{C5})$$

We know that strong convergence (a proven property of the SB space) implies pointwise converge which yields,

$$\mathbf{e}_a(z) = \sum_h v_h^*(a) v_h(z), \quad (\text{C6})$$

regardless of which orthonormal basis v_h we choose. If we specify a specific basis, namely,

$$u_{[m]}(z) = \prod_k \frac{z_k^{m_k}}{\sqrt{m_k!}}, \quad (\text{C7})$$

where m_k is a monotone increasing sequence of integers, we find,

$$\mathbf{e}_a(z) = \sum_m \prod_k \frac{(a_k^* z_k)^{m_k}}{m_k!} = e^{a^* \cdot z}, \quad (\text{C8})$$

as the gaussian reproducing kernel. It is well known that the gaussian kernel, expanded into a power series in the inner product of our data space, has positive coefficients. As such, the SB space is an RKHS with a universal kernel. This is useful as gaussian kernels are the foundation of classical machine learning and through the SB space, our quantum kernel has direct access to this kernel [46, 47].

Appendix D: A useful integral

In this section we will calculate the integral

$$I_n(a, b) := \int_{-\infty}^{\infty} dx \exp(-ax^2 + bx) x^n \quad (\text{D1})$$

for $a, b \in \mathbb{C}$ with $\text{Re}(a) > 0$ and $n \in \mathbb{N}_0$. Since CV quantum states, when represented as holomorphic functions, are always a product of a Gaussian and a polynomial, the evaluation of any CV quantum kernel will require the evaluation of integrals of the form of Eq. (D1).

1. Calculating $I_n(a, b)$

The explicit evaluation of Eq. (D1) is

$$\begin{aligned} I_n(a, b) &:= \int_{-\infty}^{\infty} dx \exp(-ax^2 + bx) x^n \\ &= a^{-(n+1)/2} \left[\frac{1 + (-1)^n}{2} \Gamma\left(\frac{1}{2} + \frac{n}{2}\right) {}_1F_1\left(\frac{1}{2} + \frac{n}{2}; \frac{1}{2}; \frac{b^2}{4a}\right) \right. \\ &\quad \left. + \frac{1 + (-1)^{n+1}}{2} \Gamma\left(\frac{3}{2} + \frac{n-1}{2}\right) \frac{b}{\sqrt{a}} {}_1F_1\left(\frac{3}{2} + \frac{n-1}{2}; \frac{3}{2}; \frac{b^2}{4a}\right) \right] \end{aligned} \quad (\text{D2})$$

where ${}_1F_1$ is the confluent hypergeometric function, which have the property that for $n \in \mathbb{N}_0$:

$${}_1F_1(b+n; b; \zeta) = e^\zeta \sum_{j=0}^n \binom{n}{j} \frac{\zeta^j}{(b)_j} \quad (\text{D3})$$

where $(b)_j$ is the Pochhammer symbol

$$(b)_j := \frac{\Gamma(b+j)}{\Gamma(b)}.$$

We explicitly prove this in section D 2.

By considering the cases of even n and odd n separately, Eq. (D3) can be used to simplify Eq. (D2) and write it as a product of a Gaussian and a polynomial.

When n is even:

$$\begin{aligned} I_n(a, b) &= a^{-(n+1)/2} \Gamma\left(\frac{1}{2} + \frac{n}{2}\right) {}_1F_1\left(\frac{1}{2} + \frac{n}{2}; \frac{1}{2}; \frac{b^2}{4a}\right) \\ &= a^{-(n+1)/2} \Gamma\left(\frac{1}{2} + \frac{n}{2}\right) \exp\left(\frac{b^2}{4a}\right) \sum_{j=0}^{n/2} \binom{n/2}{j} \frac{1}{2^{2j}(1/2)_j} \left(\frac{b}{\sqrt{a}}\right)^{2j} \\ &= a^{-(n+1)/2} \exp\left(\frac{b^2}{4a}\right) \sum_{k=0}^n \gamma_{n,k}^{(\text{even})} \left(\frac{b}{\sqrt{a}}\right)^k \end{aligned} \quad (\text{D4})$$

where

$$\gamma_{n,k}^{(\text{even})} := \begin{cases} \Gamma\left(\frac{1}{2} + \frac{n}{2}\right) \binom{n/2}{k/2} \frac{1}{2^{k(1/2)_{k/2}}}, & k \text{ even} \\ 0, & k \text{ odd} \end{cases} \quad (\text{D5})$$

and when n is odd:

$$\begin{aligned}
I_n(a, b) &= a^{-(n+1)/2} \Gamma\left(\frac{3}{2} + \frac{n-1}{2}\right) \frac{b}{\sqrt{a}} {}_1F_1\left(\frac{3}{2} + \frac{n-1}{2}; \frac{3}{2}; \frac{b^2}{4a}\right) \\
&= a^{-(n+1)/2} \Gamma\left(\frac{3}{2} + \frac{n-1}{2}\right) \exp\left(\frac{b^2}{4a}\right) \sum_{j=0}^{(n-1)/2} \binom{(n-1)/2}{j} \frac{1}{2^{2j}(3/2)_j} \left(\frac{b}{\sqrt{a}}\right)^{2j+1} \\
&= a^{-(n+1)/2} \exp\left(\frac{b^2}{4a}\right) \sum_{k=0}^n \gamma_{n,k}^{(\text{odd})} \left(\frac{b}{\sqrt{a}}\right)^k
\end{aligned} \tag{D6}$$

where

$$\gamma_{n,k}^{(\text{odd})} := \begin{cases} \Gamma\left(\frac{3}{2} + \frac{n-1}{2}\right) \binom{(n-1)/2}{(k-1)/2} \frac{1}{2^{k-1}(3/2)_{(k-1)/2}}, & k \text{ odd} \\ 0, & k \text{ even.} \end{cases} \tag{D7}$$

Therefore, combining Eqns. (D6) and (D4) gives the general result:

$$I_n(a, b) = a^{-(n+1)/2} \exp\left(\frac{b^2}{4a}\right) \sum_{j=0}^n \gamma_{n,j} \left(\frac{b}{\sqrt{a}}\right)^j \tag{D8}$$

where

$$\gamma_{n,j} := \begin{cases} \Gamma\left(\frac{1}{2} + \frac{n}{2}\right) \binom{n/2}{j/2} \frac{1}{2^j(1/2)_{j/2}}, & n, j \text{ even} \\ \Gamma\left(\frac{3}{2} + \frac{n-1}{2}\right) \binom{(n-1)/2}{(j-1)/2} \frac{1}{2^{j-1}(3/2)_{(j-1)/2}}, & n, j \text{ odd} \\ 0, & \text{otherwise.} \end{cases} \tag{D9}$$

2. Writing ${}_1F_1(b+n; b; \zeta)$ as a product of elementary functions

In this section, we explicitly prove Eq. (D3) and show a hypergeometric function of the form ${}_1F_1(b+n; b; \zeta)$ can be written as a product of an exponential and a polynomial of degree n .

This proof requires two properties of hypergeometric functions[48, (13.6.1),(13.3.4)]

$${}_1F_1(b; b; \zeta) = e^\zeta \tag{D10a}$$

$${}_1F_1(a; b; \zeta) = {}_1F_1(a-1; b; \zeta) + \frac{\zeta}{b} {}_1F_1(a; b+1; \zeta). \tag{D10b}$$

Proposition: For $n \in \mathbb{N}_0$, the confluent hypergeometric function

$${}_1F_1(b+n; b; \zeta) = e^\zeta \sum_{j=0}^n \binom{n}{j} \frac{\zeta^j}{(b)_j} \tag{D11}$$

where $(b)_j$ is the Pochhammer symbol.

Proof (by induction):

The base case for $n = 0$ is given in Eq. (D10a).

Assume that Eq. (D11) holds for n and consider the $n + 1$ case

$$\begin{aligned}
{}_1F_1(b+n+1; b; \zeta) &= {}_1F_1(b+n; b; \zeta) + \frac{\zeta}{b} {}_1F_1(b+n+1; b+1; \zeta) \\
&= e^\zeta \sum_{j=0}^n \binom{n}{j} \frac{\zeta^j}{(b)_j} + \frac{\zeta}{b} \left(e^\zeta \sum_{j=0}^n \binom{n}{j} \frac{\zeta^j}{(b+1)_j} \right) \\
&= e^\zeta \left(\sum_{j=0}^n \binom{n}{j} \frac{\zeta^j}{(b)_j} + \sum_{j=0}^n \binom{n}{j} \frac{\Gamma(b+1)}{\Gamma(b+j+1)} \frac{\zeta^{j+1}}{b} \right) \\
&= e^\zeta \left(\sum_{j=0}^n \binom{n}{j} \frac{\zeta^j}{(b)_j} + \sum_{k=1}^{n+1} \binom{n}{k-1} \frac{\Gamma(b)}{\Gamma(b+k)} \zeta^k \right) \\
&= e^\zeta \left(1 + \sum_{j=1}^n \binom{n}{j} \frac{\zeta^j}{(b)_j} + \sum_{j=1}^n \binom{n}{j-1} \frac{\zeta^j}{(b)_j} + \frac{\zeta^{n+1}}{(b)_n} \right) \\
&= e^\zeta \left(1 + \sum_{j=1}^n \binom{n+1}{j} \frac{\zeta^j}{(b)_j} + \frac{\zeta^{n+1}}{(b)_n} \right) \quad (\text{Pascal's identity}) \\
&= e^\zeta \sum_{j=0}^{n+1} \binom{n+1}{j} \frac{\zeta^j}{(b)_j}. \tag{D12}
\end{aligned}$$

Therefore if Eq. (D11) holds for n then it holds for $n + 1$.

By the induction rule, Eq. (D11) holds for all $n \in \mathbb{N}_0$. \square

Appendix E: Details of the displaced Fock state kernel

In this section we show the details of the derivation and properties of the displaced Fock state kernel (Eq. (26)).

1. Derivation of Eq. (26)

The displaced Fock state inner product is calculated from Eq. (25) by first setting $z = x + iy$ and applying the trinomial expansion so that the x and y integrals can be written in the form of Eq. (D8).

$$\begin{aligned}
\langle F_\alpha^\star(z) | F_\beta^\star(z) \rangle &= \frac{1}{\pi} \frac{e^{-(|\alpha|^2+|\beta|^2)/2}}{n!} \int_{-\infty}^{\infty} dx \int_{-\infty}^{\infty} dy e^{-(x^2+y^2)+\alpha^*(x-iy)+\beta(x+iy)} \\
&\quad \times (x-iy-\alpha)^n (x+iy-\beta^*)^n \\
&= \frac{1}{\pi} \frac{e^{-(|\alpha|^2+|\beta|^2)/2}}{n!} \int_{-\infty}^{\infty} dx \int_{-\infty}^{\infty} dy e^{-x^2+(\alpha^*+\beta)x} e^{-y^2-i(\alpha^*-\beta)y} \\
&\quad \times \left(\sum_{i=0}^n \sum_{j=0}^{n-i} \frac{n!}{i!j!(n-i-j)!} x^i (-iy)^j (-\alpha)^{n-i-j} \right) \\
&\quad \times \left(\sum_{k=0}^n \sum_{\ell=0}^{n-k} \frac{n!}{k!\ell!(n-k-\ell)!} x^k (iy)^\ell (-\beta^*)^{n-k-\ell} \right) \\
&= \frac{n!}{\pi} e^{-(|\alpha|^2+|\beta|^2)/2} \sum_{i=0}^n \sum_{j=0}^{n-i} \sum_{k=0}^n \sum_{\ell=0}^{n-k} \frac{(-i)^j (-\alpha)^{n-i-j}}{i!j!(n-i-j)!} \frac{(i)^\ell (-\beta^*)^{n-k-\ell}}{k!\ell!(n-k-\ell)!} \\
&\quad \times \left(\int_{-\infty}^{\infty} dx e^{-x^2+(\alpha^*+\beta)x} x^{i+k} \right) \left(\int_{-\infty}^{\infty} dy e^{-y^2-i(\alpha^*-\beta)y} y^{j+\ell} \right) \\
&= \frac{n!}{\pi} e^{-(|\alpha|^2+|\beta|^2)/2} \sum_{i=0}^n \sum_{j=0}^{n-i} \sum_{k=0}^n \sum_{\ell=0}^{n-k} \frac{(-i)^j (-\alpha)^{n-i-j}}{i!j!(n-i-j)!} \frac{(i)^\ell (-\beta^*)^{n-k-\ell}}{k!\ell!(n-k-\ell)!} \\
&\quad \times I_{i+k}(1, (\alpha^* + \beta)) I_{j+\ell}(1, -i(\alpha^* - \beta))
\end{aligned} \tag{E1}$$

Now using Eq. (D8), the displacement inner product can be directly written as:

$$\begin{aligned}
\langle F_\alpha^\star(z) | F_\beta^\star(z) \rangle &= \frac{n!}{\pi} e^{-(|\alpha|^2+|\beta|^2)/2} e^{\alpha^*\beta} \sum_{i=0}^n \sum_{j=0}^{n-i} \sum_{k=0}^n \sum_{\ell=0}^{n-k} \sum_{p=0}^{i+k} \sum_{q=0}^{j+\ell} \frac{(-i)^j (-\alpha)^{n-i-j}}{i!j!(n-i-j)!} \\
&\quad \times \frac{(i)^\ell (-\beta^*)^{n-k-\ell}}{k!\ell!(n-k-\ell)!} \gamma_{(i+k),p} \gamma_{(j+\ell),q} (\alpha^* + \beta)^p (-i(\alpha^* - \beta))^q
\end{aligned} \tag{E2}$$

which is the product of a Gaussian and a polynomial of degree $2n$ in α and β .

2. Explicit examples of the displaced Fock state kernel

In this section we write down the explicit form of the first nine displacement kernels.

Initial Fock state, $ n\rangle$	Kernel function, $k(\alpha, \beta)$
$ 0\rangle$	$e^{- \alpha-\beta ^2}$
$ 1\rangle$	$e^{- \alpha-\beta ^2} (\alpha-\beta ^2 - 1)^2$
$ 2\rangle$	$\frac{e^{- \alpha-\beta ^2}}{4} (2 - 4 \alpha-\beta ^2 + \alpha-\beta ^4)^2$
$ 3\rangle$	$\frac{e^{- \alpha-\beta ^2}}{36} (-6 + 18 \alpha-\beta ^2 - 9 \alpha-\beta ^4 + \alpha-\beta ^6)^2$
$ 4\rangle$	$\frac{e^{- \alpha-\beta ^2}}{576} (24 - 96 \alpha-\beta ^2 + 72 \alpha-\beta ^4 - 16 \alpha-\beta ^6 + \alpha-\beta ^8)^2$
$ 5\rangle$	$\frac{e^{- \alpha-\beta ^2}}{14400} (-120 + 600 \alpha-\beta ^2 - 600 \alpha-\beta ^4 + 200 \alpha-\beta ^6 - 25 \alpha-\beta ^8 + \alpha-\beta ^{10})^2$
$ 6\rangle$	$\frac{e^{- \alpha-\beta ^2}}{518400} (720 - 4320 \alpha-\beta ^2 + 5400 \alpha-\beta ^4 - 2400 \alpha-\beta ^6 + 450 \alpha-\beta ^8 - 36 \alpha-\beta ^{10} + \alpha-\beta ^{12})^2$
$ 7\rangle$	$\frac{e^{- \alpha-\beta ^2}}{25401600} (-5040 + 35280 \alpha-\beta ^2 - 52920 \alpha-\beta ^4 + 29400 \alpha-\beta ^6 - 7350 \alpha-\beta ^8 + 882 \alpha-\beta ^{10} - 49 \alpha-\beta ^{12} + \alpha-\beta ^{14})^2$
$ 8\rangle$	$\frac{e^{- \alpha-\beta ^2}}{1625702400} (40320 - 322560 \alpha-\beta ^2 + 564480 \alpha-\beta ^4 - 376320 \alpha-\beta ^6 + 117600 \alpha-\beta ^8 - 18816 \alpha-\beta ^{10} + 1568 \alpha-\beta ^{12} - 64 \alpha-\beta ^{14} + \alpha-\beta ^{16})^2$

3. Showing the displaced Fock state kernel is translation invariant

A translation invariant kernel has the property that

$$k(\alpha + \mathbf{h}, \beta + \mathbf{h}) = k(\alpha, \beta). \quad (\text{E3})$$

For the case of the displaced Fock state kernel, the vector $\mathbf{h} = (h_1, h_2)^\top \in \mathbb{R}^2$, and we define $h = h_1 + ih_2$. Now the shifted kernel is

$$k(\alpha + \mathbf{h}, \beta + \mathbf{h}) = |\langle F_{\alpha+h}^*(z) | F_{\beta+h}^*(z) \rangle|^2 \quad (\text{E4})$$

where

$$\begin{aligned} & \langle F_{\alpha+h}^*(z) | F_{\beta+h}^*(z) \rangle \\ &= \frac{1}{\pi} \frac{e^{-(|\alpha+h|^2 + |\beta+h|^2)/2}}{n!} \int_{z \in \mathbb{C}} d^2z e^{-[|z|^2 - (\alpha^* + h^*)z^* - (\beta + h)z]} (z^* - \alpha - h)^n (z - \beta^* - h^*)^n. \end{aligned} \quad (\text{E5})$$

Change variables $z \rightarrow z + h^*$, so the inner product is now

$$\begin{aligned} \langle F_{\alpha+h}^*(z) | F_{\beta+h}^*(z) \rangle &= \frac{1}{\pi} \frac{e^{-(|\alpha+h|^2 + |\beta+h|^2)/2}}{n!} \int_{z \in \mathbb{C}} d^2z e^{-|z+h^*|^2 + (\alpha^* + h^*)(z^* + h) + (\beta + h)(z + h^*)} \\ &= \frac{1}{\pi} \frac{e^{-(|\alpha|^2 + |\beta|^2)/2} e^{[h(\alpha^* - \beta^*) - h^*(\alpha - \beta)]/2}}{n!} \\ &\quad \times \int_{z \in \mathbb{C}} d^2z e^{-[|z| - \alpha^* z^* - \beta z]} (z^* - \alpha)^n (z - \beta^*)^n \\ &= e^{i \text{Im}[h(\alpha^* - \beta^*)]} \langle F_\alpha^*(z) | F_\beta^*(z) \rangle. \end{aligned} \quad (\text{E6})$$

Therefore:

$$\begin{aligned} k(\alpha + \mathbf{h}, \beta + \mathbf{h}) &= |\langle F_{\alpha+h}^*(z) | F_{\beta+h}^*(z) \rangle|^2 \\ &= \left(e^{i \text{Im}[h(\alpha^* - \beta^*)]} \langle F_\alpha^*(z) | F_\beta^*(z) \rangle \right) \left(e^{-i \text{Im}[h(\alpha^* - \beta^*)]} \langle F_\alpha^*(z) | F_\beta^*(z) \rangle^* \right) \\ &= |\langle F_\alpha^*(z) | F_\beta^*(z) \rangle|^2 \\ &= k(\alpha, \beta) \end{aligned} \quad (\text{E7})$$

and the displacement kernel is translation invariant.

4. Showing the displaced Fock state kernel is rotation invariant

A rotation invariant kernel has the property that

$$k(\mathcal{R}(\theta)\alpha, \mathcal{R}(\theta)\beta) = k(\alpha, \beta). \quad (\text{E8})$$

For the case of the displaced Fock state kernel, the rotation matrix is

$$\mathcal{R}(\theta) = \begin{pmatrix} \cos(\theta) & -\sin(\theta) \\ \sin(\theta) & \cos(\theta) \end{pmatrix}. \quad (\text{E9})$$

Under this transformation, the complex number $\alpha \rightarrow e^{i\theta}\alpha$, so the rotated kernel is

$$k(\mathcal{R}(\theta)\alpha, \mathcal{R}(\theta)\beta) = \left| \left\langle F_{\exp(i\theta)\alpha}^*(z) \mid F_{\exp(i\theta)\beta}^*(z) \right\rangle \right|^2, \quad (\text{E10})$$

where

$$\begin{aligned} \left\langle F_{\exp(i\theta)\alpha}^*(z) \mid F_{\exp(i\theta)\beta}^*(z) \right\rangle &= \frac{1}{\pi} \frac{e^{-(|\alpha|^2+|\beta|^2)/2}}{n!} \int_{z \in \mathbb{C}} d^2z e^{-[|z|^2 - \exp(-i\theta)\alpha^* z^* - \exp(i\theta)\beta z]} \\ &\quad \times (z^* - e^{i\theta}\alpha)^n (z + e^{-i\theta}\beta^*)^n. \end{aligned} \quad (\text{E11})$$

Change variables $z \rightarrow e^{-i\theta}z$, so the inner product is now

$$\begin{aligned} \left\langle F_{\exp(i\theta)\alpha}^*(z) \mid F_{\exp(i\theta)\beta}^*(z) \right\rangle &= \frac{1}{\pi} \frac{e^{-(|\alpha|^2+|\beta|^2)/2}}{n!} \\ &\quad \times \int_{z \in \mathbb{C}} d^2z e^{-[|z|^2 - \exp(-i\theta)\alpha^* \exp(i\theta)z^* - \exp(i\theta)\beta \exp(-i\theta)z]} \\ &\quad \times (e^{i\theta}z^* - e^{i\theta}\alpha)^n (e^{-i\theta}z + e^{-i\theta}\beta^*)^n \\ &= \frac{1}{\pi} \frac{e^{-(|\alpha|^2+|\beta|^2)/2}}{n!} \int_{z \in \mathbb{C}} d^2z e^{-(|z|^2 - \alpha^* z^* - \beta z)} \\ &\quad \times e^{ni\theta} e^{-ni\theta} (z^* - \alpha)^n (z + \beta^*)^n \\ &= \frac{1}{\pi} \frac{e^{-(|\alpha|^2+|\beta|^2)/2}}{n!} \int_{z \in \mathbb{C}} d^2z e^{-(|z|^2 - \alpha^* z^* - \beta z)} \\ &\quad \times (z^* - \alpha)^n (z + \beta^*)^n \\ &= \langle F_\alpha^*(z) \mid F_\beta^*(z) \rangle \end{aligned} \quad (\text{E12})$$

and the displaced Fock state kernel is rotational invariant.

5. Showing the displaced Fock state kernel is a radial kernel

From these translation and rotation invariance of the displaced Fock state kernel, can also show that

$$\begin{aligned} k(\mathcal{R}(\theta)(\alpha - \beta)) &= k(\mathcal{R}(\theta)\alpha - \mathcal{R}(\theta)\beta) \\ &= k(\mathcal{R}(\theta)\alpha, \mathcal{R}(\theta)\beta) \\ &= k(\alpha, \beta) \\ &= k(\alpha - \beta), \end{aligned} \quad (\text{E13})$$

and therefore

$$k(\alpha, \beta) = k(|\alpha - \beta|) \quad (\text{E14})$$

it is a radial kernel.

Furthermore, the polynomial $P(\alpha, \beta)$ is a polynomial of α_1 , α_2 , β_1 and β_2 , but, there is no way of constructing

$$|\mathbf{s}| = \sqrt{(\alpha_1 - \beta_1)^2 + (\alpha_2 - \beta_2)^2} \quad (\text{E15})$$

out of such a polynomial. However there is a way of constructing

$$|\mathbf{s}|^2 = (\alpha_1 - \beta_1)^2 + (\alpha_2 - \beta_2)^2 = \alpha_1^2 + \alpha_2^2 + \beta_1^2 + \beta_2^2 - 2\alpha_1\beta_1 - 2\alpha_2\beta_2 \quad (\text{E16})$$

and therefore

$$k(\boldsymbol{\alpha}, \boldsymbol{\beta}) = k(|\boldsymbol{\alpha} - \boldsymbol{\beta}|^2) \quad (\text{E17})$$

6. The Fourier transform of the displaced Fock state kernel

Now define $\mathbf{s} := \boldsymbol{\alpha} - \boldsymbol{\beta}$, and use the facts that the displaced Fock state kernel is

$$k(\boldsymbol{\alpha}, \boldsymbol{\beta}) = k(|\mathbf{s}|^2) \quad (\text{E18})$$

and is the product of a Gaussian and a polynomial of degree $4n$ in \mathbf{s} , to write is as

$$k(|\mathbf{s}|) = e^{-|\mathbf{s}|^2} \sum_{j=0}^{2n} a_{2j} |\mathbf{s}|^{2j} \quad (\text{E19})$$

for an appropriate choice of $a_j \in \mathbb{R}$.

The two-dimensional Fourier transform can be easily calculated as

$$\begin{aligned} \frac{1}{2\pi} \int d^2s \, e^{i\mathbf{s} \cdot \boldsymbol{\omega}} k(\mathbf{s}) &= \frac{1}{2\pi} \sum_{j=0}^{2n} a_{2j} \int_0^\infty ds \int_0^{2\pi} d\theta \, s e^{is\omega \cos(\theta)} e^{-s^2} s^{2j} \\ &= \frac{1}{2\pi} \sum_{j=0}^{2n} a_{2j} \int_0^\infty ds \, e^{-s^2} s^{2j+1} J_0(\omega s) \\ &= \frac{1}{2\pi} \sum_{j=0}^{2n} a_{2j} \left[\frac{j!}{2} {}_1F_1 \left(1+j; 1; -\frac{\omega^2}{4} \right) \right] \end{aligned} \quad (\text{E20})$$

which can be simplified further using the hypergeometric identity in appendix D 2

$$\begin{aligned} \frac{1}{2\pi} \int d^2s \, e^{i\mathbf{s} \cdot \boldsymbol{\omega}} k(\mathbf{s}) &= \frac{1}{4\pi} \sum_{j=0}^{2n} j! \, a_{2j} \, e^{-\omega^2/4} \sum_{\ell=0}^j \binom{j}{\ell} \frac{1}{(1)_\ell} \left(-\frac{\omega^2}{4} \right)^\ell \\ &= \frac{e^{-\omega^2/4}}{4\pi} \sum_{j=0}^{2n} (j!)^2 a_{2j} \sum_{\ell=0}^j \frac{(-1)^\ell}{(\ell!)^2 (j-\ell)!} \left(\frac{\omega}{2} \right)^{2\ell} \end{aligned} \quad (\text{E21})$$

which is also the product of a Gaussian and a polynomial of degree $4n$ in ω .

7. Showing the displaced Fock state kernel integrates to π

In this section, we calculate the displaced Fock state kernel from the operator definition:

$$\hat{D}(\alpha) = e^{\alpha \hat{a}^\dagger - \alpha^* \hat{a}} = e^{-|\alpha|^2/2} e^{\alpha \hat{a}^\dagger} e^{-\alpha^* \hat{a}}. \quad (\text{E22})$$

Starting from

$$\begin{aligned} e^{\pm \alpha^* \hat{a}} |n\rangle &= \sum_{j=0}^{\infty} \frac{(\pm \alpha^*)^j \hat{a}^j}{j!} |n\rangle \\ &= |n\rangle + \sum_{j=1}^{\infty} \frac{(\pm \alpha^*)^j \hat{a}^j}{j!} |n\rangle \\ &= |n\rangle + \sum_{j=1}^n \frac{(\pm \alpha^*)^j}{j!} \prod_{\ell=1}^j \sqrt{n-\ell+1} |n-j\rangle. \end{aligned} \quad (\text{E23})$$

we calculate the inner product as

$$\begin{aligned}
\langle n | \hat{D}^\dagger(\alpha) \hat{D}(\beta) | n \rangle &= e^{(-\alpha\beta^* + \alpha^*\beta)/2} \langle n | \hat{D}(\beta - \alpha) | n \rangle \\
&= e^{-|\beta - \alpha|^2/2} e^{i \operatorname{Im}(\alpha^*\beta)} \langle n | e^{(\beta - \alpha)\hat{a}^\dagger} e^{-(\beta - \alpha)^*\hat{a}} | n \rangle \\
&= e^{-|\beta - \alpha|^2/2} e^{i \operatorname{Im}(\alpha^*\beta)} \left(e^{(\beta - \alpha)^*\hat{a}} | n \rangle \right)^\dagger \left(e^{-(\beta - \alpha)\hat{a}} | n \rangle \right) \\
&= e^{-|\beta - \alpha|^2/2} e^{i \operatorname{Im}(\alpha^*\beta)} \left(\langle n | + \sum_{i=1}^n \frac{(\beta - \alpha)^i}{i!} \prod_{k=1}^i \sqrt{n - k + 1} \langle n - i | \right) \\
&\quad \times \left(| n \rangle + \sum_{j=1}^n \frac{-(\beta - \alpha)^*}{j!} \prod_{\ell=1}^j \sqrt{n - \ell + 1} | n - j \rangle \right) \\
&= e^{-|\beta - \alpha|^2/2} e^{i \operatorname{Im}(\alpha^*\beta)} \left(1 + \sum_{j=1}^n \frac{(\beta - \alpha)^j (-(\beta - \alpha)^*)^j}{(j!)^2} \left(\sqrt{n} \sqrt{n-1} \dots \sqrt{n-j+1} \right)^2 \right) \\
&= e^{-|\beta - \alpha|^2/2} e^{i \operatorname{Im}(\alpha^*\beta)} \sum_{j=0}^n \frac{(-1)^j |\beta - \alpha|^{2j}}{(j!)^2} \frac{n!}{(n-j)!} \\
&= e^{-|\beta - \alpha|^2/2} e^{i \operatorname{Im}(\alpha^*\beta)} \sum_{j=0}^n \binom{n}{j} \frac{(-1)^j |\beta - \alpha|^{2j}}{j!}
\end{aligned} \tag{E24}$$

and the displaced Fock state kernel

$$k(\alpha, \beta) = \left| \langle n | \hat{D}^\dagger(\alpha) \hat{D}(\beta) | n \rangle \right|^2 = e^{-|\beta - \alpha|^2} \left(\sum_{j=0}^n \binom{n}{j} \frac{(-1)^j |\beta - \alpha|^{2j}}{j!} \right)^2. \tag{E25}$$

Note that this is a much simpler form than that which we found Eq. (26), indicating that there may be a way to significantly simplify the general multi-mode kernel Eq. (46). We leave this exploration for future work.

Now define $\mathbf{s} := \alpha - \beta \in \mathbb{R}^2$ and integrate the kernel over all \mathbf{s}

$$\begin{aligned}
\int d^2s \, k(|\mathbf{s}|) &= \int_0^\infty ds \, s \int_0^{2\pi} d\theta \, e^{-s^2} \left(\sum_{j=0}^n \binom{n}{j} \frac{(-1)^j s^{2j}}{j!} \right)^2 \\
&= 2\pi \sum_{j=0}^n \sum_{k=0}^n \binom{n}{j} \binom{n}{k} \frac{(-1)^j}{j!} \frac{(-1)^k}{k!} \int_0^\infty ds \, e^{-s^2} s^{2(j+k)+1} \\
&= 2\pi \sum_{j=0}^n \sum_{k=0}^n \binom{n}{j} \binom{n}{k} \frac{(-1)^{j+k}}{j!k!} \left(\frac{\Gamma(1+j+k)}{2} \right) \\
&= \pi \sum_{j=0}^n \sum_{k=0}^n (-1)^{j+k} \binom{n}{j} \binom{n}{k} \binom{j+k}{k}.
\end{aligned} \tag{E26}$$

The binomial coefficients can be further simplified by using the following properties for $k, n \in \mathbb{N}_0$, $m \in \mathbb{Z}$, and $x, y \in \mathbb{R}$ [49]:

$$\binom{x}{k} = \frac{x^{\underline{k}}}{k!} \tag{E27a}$$

$$\binom{m}{k} = (-1)^k \binom{-m+k-1}{k} \tag{E27b}$$

$$\binom{n}{k} = (-1)^{n-k} \binom{-k-1}{n-k} \quad k \leq n \tag{E27c}$$

$$\binom{x+y}{n} = \sum_{k=0}^n \binom{x}{k} \binom{y}{n-k} \tag{E27d}$$

where

$$x^{\underline{k}} = x(x-1)(x-2)\dots(x-k+1) \quad (\text{E28})$$

is the falling factorial.

With these properties, the integral becomes:

$$\begin{aligned} \int d^2s \, k(|\mathbf{s}|) &= \pi \sum_{j=0}^n \sum_{k=0}^n (-1)^{j+k} \binom{n}{j} \binom{n}{k} \binom{j+k}{k} \\ &= \pi \sum_{j=0}^n \sum_{k=0}^n (-1)^{j+k} \binom{n}{j} \binom{n}{k} (-1)^{j+k-k} \binom{-(k+1)}{j} \quad (\text{Eq. (E27c)}) \\ &= \pi \sum_{k=0}^n (-1)^k \binom{n}{k} \sum_{j=0}^n \binom{n}{n-j} \binom{-(k+1)}{j} \\ &= \pi \sum_{k=0}^n (-1)^k \binom{n}{k} \binom{n-(k+1)}{n} \quad (\text{Eq. (E27d)}) \\ &= \pi \sum_{k=0}^n (-1)^k \binom{n}{k} (-1)^n \binom{k}{n} \quad (\text{Eq. (E27b)}) \\ &= \pi \sum_{k=0}^n (-1)^{n+k} \binom{n}{k} \frac{k^n}{n!} \quad (\text{Eq. (E27a)}). \quad (\text{E29}) \end{aligned}$$

Since $0 \leq k \leq n$, the falling factorial becomes

$$k^{\underline{n}} = k(k-1)\dots(k-k)\dots(k-n+1) \quad (\text{E30})$$

which is zero unless $k = n$, so

$$\begin{aligned} \int d^2s \, k(|\mathbf{s}|) &= \pi \sum_{k=0}^n (-1)^{n+k} \binom{n}{k} \frac{k(k-1)\dots(k-n+1)}{n!} \delta_{k,n} \\ &= \pi (-1)^{2n} \binom{n}{n} \frac{n!}{n!} \\ &= \pi \quad (\text{E31}) \end{aligned}$$

for all $n \in \mathbb{N}_0$.

Appendix F: Explicit calculation of the general m -mode kernel

In this section, we provide the details of the calculation of the general m -mode kernel (Eq. (46)).

The first step in calculating the m -mode kernel is to rewrite Eq. (44) to become a series of nested integrals each of the form of Eq. (D8).

Starting from the general m -mode inner product,

$$\begin{aligned}
\langle F_{x_1}^* | F_{x_2}^* \rangle &= \frac{1}{\pi^m} \int_{\mathbf{z} \in \mathbb{C}^m} d^{2m} z e^{-|z|^2} F_{x_1}(\mathbf{z})^* F_{x_2}(\mathbf{z}) \\
&= \frac{1}{\pi^m} \int_{\mathbf{z} \in \mathbb{C}^m} d^{2m} z e^{-|z|^2} \exp \left(-\frac{1}{2} \mathbf{z}^\dagger A^{(1)*} \mathbf{z}^* + B^{(1)\dagger} \mathbf{z}^* + C^{(1)*} \right) \\
&\quad \times \left(\sum_{i_1+i_2+\dots+i_m=n} \beta_{\mathbf{i}}^{(1)*} (z_1^*)^{i_1} (z_2^*)^{i_2} \dots (z_n^*)^{i_n} \right) \\
&\quad \times \exp \left(-\frac{1}{2} \mathbf{z}^\top A^{(2)} \mathbf{z} + B^{(2)\top} \mathbf{z} + C^{(2)} \right) \left(\sum_{j_1+j_2+\dots+j_n=n} \beta_{\mathbf{j}}^{(2)} z_1^{j_1} z_2^{j_2} \dots z_n^{j_n} \right) \\
&= \frac{1}{\pi^m} \int_{\mathbf{z} \in \mathbb{C}^m} d^{2m} \exp \left(-|z|^2 - \frac{1}{2} \mathbf{z}^\dagger A^{(1)*} \mathbf{z}^* - \frac{1}{2} \mathbf{z}^\top A^{(2)} \mathbf{z} + B^{(1)\dagger} \mathbf{z}^* + B^{(2)\top} \mathbf{z} + C^{(1)*} + C^{(2)} \right) \\
&\quad \times \left(\sum_{i_1+i_2+\dots+i_m=n} \sum_{j_1+j_2+\dots+j_n=n} \beta_{\mathbf{i}}^{(1)*} \beta_{\mathbf{j}}^{(2)} (z_1^*)^{i_1} z_1^{j_1} (z_2^*)^{i_2} z_2^{j_2} \dots (z_n^*)^{i_n} z_n^{j_n} \right). \tag{F1}
\end{aligned}$$

Unsurprisingly the integrand is also of the form

$$\exp [Q(\mathbf{z})] \times P(\mathbf{z}) \tag{F2}$$

i.e. the product of a Gaussian and a polynomial.

Similar to the calculation of the displaced Fock state kernel, we set $z_j = x_{2j-1} + i x_{2j}$ for each $j \in [1, m]$. After some algebra, which we detail below, this substitution will allow for Eq. (F1) to be written as a nested set of integrals, each of the form of Eq. (D8).

First simplify the Gaussian part of the integrand:

$$\begin{aligned}
Q(\mathbf{z}) &= \left(C^{(1)*} + C^{(2)} \right) + \sum_{j=1}^m - (x_{2j-1}^2 + x_{2j}^2) - \frac{A_{j,j}^{(1)*}}{2} (x_{2j-1} - i x_{2j})^2 - \frac{A_{j,j}^{(2)}}{2} (x_{2j-1} + i x_{2j})^2 \\
&\quad + (x_{2j-1} - i x_{2j}) \left(B_j^{(1)*} - \sum_{k=j+1}^m \frac{A_{j,k}^{(1)*} + A_{k,j}^{(1)*}}{2} (x_{2j-1} - i x_{2j}) \right) \\
&\quad + (x_{2j-1} + i x_{2j}) \left(B_j^{(2)} - \sum_{k=j+1}^m \frac{A_{j,k}^{(2)} + A_{k,j}^{(2)}}{2} (x_{2j-1} + i x_{2j}) \right) \\
&= \left(C^{(1)*} + C^{(2)} \right) + \sum_{j=1}^m - \left(1 + \frac{A_{j,j}^{(1)*}}{2} + \frac{A_{j,j}^{(2)}}{2} \right) x_{2j-1}^2 - \left(1 - \frac{A_{j,j}^{(1)*}}{2} - \frac{A_{j,j}^{(2)}}{2} \right) x_{2j}^2 \\
&\quad + x_{2j-1} \left(\left(B_j^{(1)*} + B_j^{(2)} \right) - i \left(A_{j,j}^{(1)*} - A_{j,j}^{(2)} \right) x_{2j} \right. \\
&\quad \left. - \frac{1}{2} \sum_{k=j+1}^m \left(A_{j,k}^{(1)*} + A_{k,j}^{(1)*} + A_{j,k}^{(2)} + A_{k,j}^{(2)} \right) x_{2k-1} - i \left(A_{j,k}^{(1)*} + A_{k,j}^{(1)*} - A_{j,k}^{(2)} - A_{k,j}^{(2)} \right) x_{2k} \right) \\
&\quad - i x_{2j} \left(\left(B_j^{(1)*} - B_j^{(2)} \right) \right. \\
&\quad \left. - \frac{1}{2} \sum_{k=j+1}^m \left(A_{j,k}^{(1)*} + A_{k,j}^{(1)*} - A_{j,k}^{(2)} - A_{k,j}^{(2)} \right) x_{2k-1} - i \left(A_{j,k}^{(1)*} + A_{k,j}^{(1)*} + A_{j,k}^{(2)} + A_{k,j}^{(2)} \right) x_{2k} \right) \\
&= \left(C^{(1)*} + C^{(2)} \right) + \sum_{j=1}^{2m} -a_{0,j} x_j^2 + x_j \left(b_{0,j} + \sum_{k=j+1}^{2m} d_{0,j,k} x_k \right) \tag{F3}
\end{aligned}$$

where for odd j

$$\begin{aligned}
a_{0,j} &:= \left(1 + \frac{\left(A_{(j+1)/2, (j+1)/2}^{(1)} \right)^*}{2} + \frac{A_{(j+1)/2, (j+1)/2}^{(2)}}{2} \right) \\
b_{0,j} &:= \left(B_{(j+1)/2}^{(1)} \right)^* + B_{(j+1)/2}^{(2)} \\
d_{0,j,k} &:= \begin{cases} -i \left[\left(A_{(j+1)/2, (j+1)/2}^{(1)} \right)^* - A_{(j+1)/2, (j+1)/2}^{(2)} \right], & k = j + 1 \\ -\frac{1}{2} \left[\left(A_{(j+1)/2, (k+1)/2}^{(1)} + A_{(k+1)/2, (j+1)/2}^{(1)} \right)^* + A_{(j+1)/2, (k+1)/2}^{(2)} + A_{(k+1)/2, (j+1)/2}^{(2)} \right], & k \geq j + 2, \text{ } k \text{ odd} \\ \frac{i}{2} \left[\left(A_{(j+1)/2, k/2}^{(1)} + A_{k/2, (j+1)/2}^{(1)} \right)^* - A_{(j+1)/2, k/2}^{(2)} - A_{k/2, (j+1)/2}^{(2)} \right], & k \geq j + 3, \text{ } k \text{ even} \end{cases}
\end{aligned} \tag{F4}$$

and for even j

$$\begin{aligned}
a_{0,j} &:= \left(1 - \frac{\left(A_{j/2, j/2}^{(1)} \right)^*}{2} - \frac{A_{j/2, j/2}^{(2)}}{2} \right) \\
b_{0,j} &:= -i \left[\left(B_{j/2}^{(1)} \right)^* + B_{j/2}^{(2)} \right] \\
d_{0,j,k} &:= \begin{cases} \frac{i}{2} \left[\left(A_{j/2, (k+1)/2}^{(1)} + A_{(k+1)/2, j/2}^{(1)} \right)^* - A_{j/2, (k+1)/2}^{(2)} - A_{(k+1)/2, j/2}^{(2)} \right], & k \geq j + 1, \text{ } k \text{ odd} \\ \frac{1}{2} \left[\left(A_{j/2, k/2}^{(1)} + A_{k/2, j/2}^{(1)} \right)^* + A_{j/2, k/2}^{(2)} + A_{k/2, j/2}^{(2)} \right], & k \geq j + 2, \text{ } k \text{ even.} \end{cases}
\end{aligned} \tag{F5}$$

Next, simplify the polynomial part of the integrand:

$$\begin{aligned}
P(\mathbf{z}) &= \sum_{i_1 + \dots + i_m = n} \sum_{j_1 + \dots + j_m = n} \beta_{\mathbf{i}}^{(1)*} \beta_{\mathbf{j}}^{(2)} \prod_{k=1}^m (x_{2k-1} - i x_{2k})^{i_k} (x_{2k-1} + i x_{2k})^{j_k} \\
&= \sum_{i_1 + \dots + i_m = n} \sum_{j_1 + \dots + j_m = n} \beta_{\mathbf{i}}^{(1)*} \beta_{\mathbf{j}}^{(2)} \prod_{k=1}^m \left(\sum_{p_k=0}^{i_k} \sum_{q_k=0}^{j_k} \binom{i_k}{p_k} \binom{j_k}{q_k} (-i)^{p_k} (i)^{q_k} x_{2k-1}^{i_k+j_k-p_k-q_k} x_{2k}^{p_k+q_k} \right) \\
&= \sum_{i_1 + \dots + i_m = n} \sum_{j_1 + \dots + j_m = n} \beta_{\mathbf{i}}^{(1)*} \beta_{\mathbf{j}}^{(2)} \\
&\quad \times \sum_{p_1=0}^{i_1} \sum_{q_1=0}^{j_1} \sum_{p_2=0}^{i_2} \sum_{q_2=0}^{j_2} \dots \sum_{p_m=0}^{i_m} \sum_{q_m=0}^{j_m} \prod_{k=1}^m \binom{i_k}{p_k} \binom{j_k}{q_k} (-i)^{p_k} (i)^{q_k} x_{2k-1}^{i_k+j_k-p_k-q_k} x_{2k}^{p_k+q_k} \\
&= \sum_{i_1 + \dots + i_m = n} \sum_{j_1 + \dots + j_m = n} \beta_{\mathbf{i}}^{(1)*} \beta_{\mathbf{j}}^{(2)} \sum_{\mathbf{p}=\mathbf{0}}^{\mathbf{i}} \sum_{\mathbf{q}=\mathbf{0}}^{\mathbf{j}} \prod_{k=1}^{2m} g_{0,k} x_k^{r_{0,k}}
\end{aligned} \tag{F6}$$

where

$$\begin{aligned}
\sum_{\mathbf{p}=\mathbf{0}}^{\mathbf{i}} &= \sum_{p_1=0}^{i_1} \sum_{p_2=0}^{i_2} \dots \sum_{p_m=0}^{i_m} \\
\sum_{\mathbf{q}=\mathbf{0}}^{\mathbf{j}} &= \sum_{q_1=0}^{j_1} \sum_{q_2=0}^{j_2} \dots \sum_{q_m=0}^{j_m} \\
g_{0,k} &:= \begin{cases} 1, & k \text{ odd} \\ \binom{i_{k/2}}{p_{k/2}} \binom{j_{k/2}}{q_{k/2}} (-i)^{p_{k/2}} (i)^{q_{k/2}}, & k \text{ even} \end{cases} \\
r_{0,k} &:= \begin{cases} i_{(k+1)/2} + j_{(k+1)/2} - p_{(k+1)/2} - q_{(k+1)/2}, & k \text{ odd} \\ p_{k/2} + q_{k/2}, & k \text{ even.} \end{cases}
\end{aligned} \tag{F7}$$

Therefore, the m -mode inner product can be written as:

$$\begin{aligned} \langle F_{x_1}^* | F_{x_2}^* \rangle &= \frac{e^{C^{(1)*} + C^{(2)}}}{\pi^m} \sum_{i_1 + \dots + i_m = n} \sum_{j_1 + \dots + j_m = n} \beta_i^{(1)*} \beta_j^{(2)} \sum_{p=0}^i \sum_{q=0}^j \\ &\quad \times \int_{\mathbf{x} \in \mathbb{R}^{2m}} d^{2m}x \exp \left[\sum_{j=1}^{2m} -a_{0,j} x_j^2 + x_j \left(b_{0,j} + \sum_{k=j+1}^{2M} d_{0,j,k} x_k \right) \right] \\ &\quad \times \left(\prod_{k=1}^{2m} g_{0,k} x_k^{r_{0,k}} \right) \end{aligned} \quad (F8)$$

which is in the required form.

Now we can carry out the integrations starting with the x_1 integral, which is of the form Eq. (D8):

$$\begin{aligned} \langle F_{x_1}^* | F_{x_2}^* \rangle &= \frac{e^{C^{(1)*} + C^{(2)}}}{\pi^m} \sum_{i_1 + \dots + i_m = n} \sum_{j_1 + \dots + j_m = n} \beta_i^{(1)*} \beta_j^{(2)} \\ &\quad \times \sum_{p=0}^i \sum_{q=0}^j \int_{-\infty}^{\infty} dx_{2m} \int_{-\infty}^{\infty} dx_{2m-1} \cdots \int_{-\infty}^{\infty} dx_2 \\ &\quad \times \left\{ g_{0,1} \int_{-\infty}^{\infty} dx_1 \exp \left[-a_{0,1} x_1^2 + x_1 \left(b_{0,1} + \sum_{k=2}^{2m} d_{0,1,k} x_k \right) \right] x_1^{r_{0,1}} \right\} \\ &\quad \times \exp \left[\sum_{j=2}^{2m} -a_{0,j} x_j^2 + x_j \left(b_{0,j} + \sum_{k=j+1}^{2m} d_{0,j,k} x_k \right) \right] \left(\prod_{k=2}^{2m} g_{0,k} x_k^{r_{0,k}} \right) \\ &= \frac{e^{C^{(1)*} + C^{(2)}}}{\pi^m} \sum_{i_1 + \dots + i_m = n} \sum_{j_1 + \dots + j_m = n} \beta_i^{(1)*} \beta_j^{(2)} \\ &\quad \times \sum_{p=0}^i \sum_{q=0}^j \int_{-\infty}^{\infty} dx_{2m} \int_{-\infty}^{\infty} dx_{2m-1} \cdots \int_{-\infty}^{\infty} dx_2 \\ &\quad \times \left\{ g_{0,1} a_{0,1}^{-(r_{0,1}+1)/2} \exp \left[\frac{1}{4a_{0,1}} \left(b_{0,1} + \sum_{k=2}^{2m} d_{0,1,k} x_k \right)^2 \right] \right. \\ &\quad \times \left. \sum_{s_1=0}^{r_{0,1}} \gamma_{r_{0,1}, s_1} \left[\frac{1}{\sqrt{a_{0,1}}} \left(b_{0,1} + \sum_{k=2}^{2m} d_{0,1,k} x_k \right) \right]^{s_1} \right\} \\ &\quad \times \exp \left[\sum_{j=2}^{2m} -a_{0,j} x_j^2 + x_j \left(b_{0,j} + \sum_{k=j+1}^{2m} d_{0,j,k} x_k \right) \right] \left(\prod_{k=2}^{2m} g_{0,k} x_k^{r_{0,k}} \right) \\ &= \frac{e^{C^{(1)*} + C^{(2)}}}{\pi^m} \sum_{i_1 + \dots + i_m = n} \sum_{j_1 + \dots + j_m = n} \beta_i^{(1)*} \beta_j^{(2)} \\ &\quad \times \sum_{p=0}^i \sum_{q=0}^j \int_{-\infty}^{\infty} dx_{2m} \int_{-\infty}^{\infty} dx_{2m-1} \cdots \int_{-\infty}^{\infty} dx_2 \exp \left[\frac{1}{4a_{0,1}} \left(b_{0,1} + \sum_{k=2}^{2m} d_{0,1,k} x_k \right)^2 \right] \\ &\quad \times \exp \left[\sum_{j=2}^{2m} -a_{0,j} x_j^2 + x_j \left(b_{0,j} + \sum_{k=j+1}^{2m} d_{0,j,k} x_k \right) \right] \\ &\quad \times \left[a_{0,1}^{-(r_{0,1}+1)/2} \sum_{s_1=0}^{r_{0,1}} \gamma_{r_{0,1}, s_1} \left[\frac{1}{\sqrt{a_{0,1}}} \left(b_{0,1} + \sum_{k=2}^{2m} d_{0,1,k} x_k \right) \right]^{s_1} \right] \left(\prod_{k=2}^{2m} g_{0,k} x_k^{r_{0,k}} \right) \end{aligned} \quad (F9)$$

where we also use the fact that $g_{0,1} = 1$ (Eq. (F7)).

Next, the goal is to simplify the integrand so that the x_2 integral is of the form of Eq. (D8).

Start by simplifying the exponential part:

$$\begin{aligned}
& \frac{1}{4a_{0,1}} \left(b_{0,1} + \sum_{j=2}^{2m} d_{0,1,j} x_j \right)^2 + \sum_{j=2}^{2m} -a_{0,j} x_j^2 + x_j \left(b_{0,j} + \sum_{k=j+1}^{2m} d_{0,j,k} x_k \right) \\
&= \frac{b_{0,1}^2}{4a_{0,1}} + \sum_{j=2}^{2m} - \left(a_{0,j} - \frac{d_{0,1,j}^2}{4a_{0,1}} \right) x_j^2 + x_j \left[\left(b_{0,j} + \frac{b_{0,1} d_{0,1,j}}{2a_{0,1}} \right) \right. \\
&\quad \left. + \sum_{k=j+1}^{2m} \left(d_{0,j,k} + \frac{d_{0,1,j} d_{0,1,k}}{2a_{0,1}} \right) x_k \right] \\
&= \frac{b_{0,1}^2}{4a_{0,1}} + \sum_{j=2}^{2m} -a_{1,j} x_j^2 + x_j \left(b_{1,j} + \sum_{k=j+1}^{2m} d_{1,j,k} x_k \right)
\end{aligned} \tag{F10}$$

where

$$\begin{aligned}
a_{1,j} &:= a_{0,j} - \frac{d_{0,1,j}^2}{4a_{0,1}} \\
b_{1,j} &:= b_{0,j} + \frac{b_{0,1} d_{0,1,j}}{2a_{0,1}} \\
d_{1,j,k} &:= d_{0,j,k} + \frac{d_{0,1,j} d_{0,1,k}}{2a_{0,1}}.
\end{aligned} \tag{F11}$$

Then use the multinomial expansion,

$$(x_1 + x_2 + \dots + x_m)^n = \sum_{\substack{i_1, i_2, \dots, i_m \geq 0 \\ i_1 + i_2 + \dots + i_m = n}} \frac{n!}{i_1! i_2! \dots i_m!} x_1^{i_1} x_2^{i_2} \dots x_m^{i_m} \tag{F12}$$

to simplify the polynomial part:

$$\begin{aligned}
& \left[a_{0,1}^{-(r_{0,1}+1)/2} \sum_{s_1=0}^{r_{0,1}} \gamma_{r_{0,1}, s_1} \left(\frac{1}{\sqrt{a_{0,1}}} \right)^{s_1} \left(b_{0,1} + \sum_{j=2}^{2m} d_{0,1,j} x_j \right)^{s_1} \right] \left(\prod_{k=2}^{2m} g_{0,k} x_k^{r_{0,k}} \right) \\
&= \left[\sum_{s_1=0}^{r_{0,1}} \frac{\gamma_{r_{0,1}, s_1}}{a_{0,1}^{(r_{0,1}+s_1+1)/2}} \sum_{t_1=0}^{s_1} \binom{s_1}{t_1} b_{0,1}^{s_1-t_1} \left(\sum_{j=2}^{2m} d_{0,1,j} x_j \right)^{t_1} \right] \left(\prod_{k=2}^{2m} g_{0,k} x_k^{r_{0,k}} \right) \\
&= \left[\sum_{s_1=0}^{r_{0,1}} \frac{\gamma_{r_{0,1}, s_1}}{a_{0,1}^{(r_{0,1}+s_1+1)/2}} \sum_{t_1=0}^{s_1} \binom{s_1}{t_1} b_{0,1}^{s_1-t_1} \right. \\
&\quad \times \left(\sum_{u_{1,2}+u_{1,3}+\dots+u_{1,2m}=t_1} \frac{t_1!}{u_{1,2}! u_{1,3}! \dots u_{1,2m}!} \prod_{k=2}^{2m} d_{0,1,k}^{u_{1,k}} x_k^{u_{1,k}} \right) \left. \right] \\
&\quad \times \left(\prod_{k=2}^{2m} g_{0,k} x_k^{r_{0,k}} \right) \\
&= \sum_{s_1=0}^{r_{0,1}} \frac{\gamma_{r_{0,1}, s_1}}{a_{0,1}^{(r_{0,1}+s_1+1)/2}} \sum_{t_1=0}^{s_1} \frac{s_1!}{(s_1-t_1)!} b_{0,1}^{s_1-t_1} \sum_{u_{1,2}+\dots+u_{1,2m}=t_1} \prod_{k=2}^{2m} \frac{g_{0,k} d_{0,1,k}^{u_{1,k}}}{u_{1,k}!} x_k^{u_{1,k}+r_{0,k}} \\
&= \sum_{s_1=0}^{r_{0,1}} \frac{\gamma_{r_{0,1}, s_1}}{a_{0,1}^{(r_{0,1}+s_1+1)/2}} \sum_{t_1=0}^{s_1} \frac{s_1!}{(s_1-t_1)!} b_{0,1}^{s_1-t_1} \sum_{u_{1,2}+\dots+u_{1,2m}=t_1} \prod_{k=2}^{2m} g_{1,k} x_k^{r_{1,k}}
\end{aligned} \tag{F13}$$

where for $k \geq 2$

$$\begin{aligned} g_{1,k} &:= \frac{g_{0,k} d_{0,1,k}^{u_{1,k}}}{u_{1,k}!} \\ r_{1,k} &:= r_{0,k} + u_{1,k} \end{aligned} \tag{F14}$$

Therefore the m -mode inner product becomes

$$\begin{aligned} \langle F_{x_1}^* | F_{x_2}^* \rangle &= \exp \left(C^{(1)*} + C^{(2)} + \frac{b_{0,1}^2}{4a_{0,1}} \right) \sum_{i_1+\dots+i_m=n} \sum_{j_1+\dots+j_m=n} \beta_{\mathbf{i}}^{(1)*} \beta_{\mathbf{j}}^{(2)} \\ &\quad \times \sum_{\mathbf{p}=\mathbf{0}}^{\mathbf{i}} \sum_{\mathbf{q}=\mathbf{0}}^{\mathbf{j}} \sum_{s_1=0}^{r_{0,1}} \frac{\gamma_{r_{0,1},s_1}}{a_{0,1}^{(r_{0,1}+s_1+1)/2}} \sum_{t_1=0}^{s_1} \frac{s_1!}{(s_1-t_1)!} b_{0,1}^{s_1-t_1} \sum_{u_{1,2}+\dots+u_{1,2m}=t_1} \\ &\quad \times \int_{-\infty}^{\infty} dx_{2m} \cdots \int_{-\infty}^{\infty} dx_2 \exp \left[\sum_{j=2}^{2m} -a_{1,j} x_j^2 + x_j \left(b_{1,j} + \sum_{k=j+1}^{2m} d_{1,j,k} x_k \right) \right] \left(\prod_{k=2}^{2m} g_{1,k} x_k^{r_{1,k}} \right) \\ &= \exp \left(C^{(1)*} + C^{(2)} + \frac{b_{0,1}^2}{4a_{0,1}} \right) \sum_{i_1+\dots+i_m=n} \sum_{j_1+\dots+j_m=n} \beta_{\mathbf{i}}^{(1)*} \beta_{\mathbf{j}}^{(2)} \\ &\quad \times \sum_{\mathbf{p}=\mathbf{0}}^{\mathbf{i}} \sum_{\mathbf{q}=\mathbf{0}}^{\mathbf{j}} \sum_{s_1=0}^{r_{0,1}} \frac{\gamma_{r_{0,1},s_1}}{a_{0,1}^{(r_{0,1}+s_1+1)/2}} \sum_{t_1=0}^{s_1} \frac{s_1!}{(s_1-t_1)!} b_{0,1}^{s_1-t_1} \sum_{u_{1,2}+\dots+u_{1,2m}=t_1} \int_{-\infty}^{\infty} dx_{2m} \cdots \int_{-\infty}^{\infty} dx_3 \\ &\quad \times \left\{ g_{1,2} \int_{-\infty}^{\infty} dx_2 \exp \left[-a_{1,2} x_2^2 + x_2 \left(b_{1,2} + \sum_{k=3}^{2m} d_{1,2,k} x_k \right) \right] x_2^{r_{1,2}} \right\} \\ &\quad \times \exp \left[\sum_{j=3}^{2m} -a_{1,j} x_j^2 + x_j \left(b_{1,j} + \sum_{k=j+1}^{2m} d_{1,j,k} x_k \right) \right] \left(\prod_{k=3}^{2m} g_{1,k} x_k^{r_{1,k}} \right) \end{aligned}$$

$$\begin{aligned}
&= \exp \left(C^{(1)*} + C^{(2)} + \frac{b_{0,1}^2}{4a_{0,1}} \right) \sum_{i_1+\dots+i_m=n} \sum_{j_1+\dots+j_m=n} \beta_{\mathbf{i}}^{(1)*} \beta_{\mathbf{j}}^{(2)} \\
&\times \sum_{\mathbf{p}=\mathbf{0}}^{\mathbf{i}} \sum_{\mathbf{q}=\mathbf{0}}^{\mathbf{j}} \sum_{s_1=0}^{r_{0,1}} \frac{\gamma_{r_{0,1},s_1}}{a_{0,1}^{(r_{0,1}+s_1+1)/2}} \sum_{t_1=0}^{s_1} \frac{s_1!}{(s_1-t_1)!} b_{0,1}^{s_1-t_1} \sum_{u_{1,2}+\dots+u_{1,2m}=t_1} \int_{-\infty}^{\infty} dx_{2m} \cdots \int_{-\infty}^{\infty} dx_3 \\
&\times \left\{ g_{1,2} a_{1,2}^{-(r_{1,2}+1)/2} \exp \left[\frac{1}{4a_{1,2}} \left(b_{1,2} + \sum_{k=3}^{2m} d_{1,2,k} x_k \right) \right]^{s_2} \right. \\
&\times \sum_{s_2=0}^{r_{1,2}} \gamma_{r_{1,2},s_2} \left[\frac{1}{\sqrt{a_{1,2}}} \left(b_{1,2} + \sum_{k=3}^{2m} d_{1,2,k} x_k \right) \right]^{s_2} \left. \right\} \\
&\times \exp \left[\sum_{j=3}^{2m} -a_{1,j} x_j^2 + x_j \left(b_{1,j} + \sum_{k=j+1}^{2m} d_{1,j,k} x_k \right) \right] \left(\prod_{k=3}^{2m} g_{1,k} x_k^{r_{1,k}} \right) \\
&= \exp \left(C^{(1)*} + C^{(2)} + \frac{b_{0,1}^2}{4a_{0,1}} + \frac{b_{1,2}^2}{4a_{1,2}} \right) \sum_{i_1+\dots+i_m=n} \sum_{j_1+\dots+j_m=n} \beta_{\mathbf{i}}^{(1)*} \beta_{\mathbf{j}}^{(2)} \\
&\times \sum_{\mathbf{p}=\mathbf{0}}^{\mathbf{i}} \sum_{\mathbf{q}=\mathbf{0}}^{\mathbf{j}} \sum_{s_1=0}^{r_{0,1}} \frac{\gamma_{r_{0,1},s_1}}{a_{0,1}^{(r_{0,1}+s_1+1)/2}} \sum_{t_1=0}^{s_1} \frac{s_1!}{(s_1-t_1)!} b_{0,1}^{s_1-t_1} \sum_{u_{1,2}+\dots+u_{1,2m}=t_1} g_{1,2} \\
&\times \sum_{s_2=0}^{r_{1,2}} \frac{\gamma_{r_{1,2},s_2}}{a_{1,2}^{(r_{1,2}+s_2+1)/2}} \sum_{t_2=0}^{s_2} \frac{s_2!}{(s_2-t_2)!} b_{1,2}^{s_2-t_2} \sum_{u_{2,3}+\dots+u_{2,2m}=t_2} \\
&\times \int_{-\infty}^{\infty} dx_{2m} \cdots \int_{-\infty}^{\infty} dx_3 \exp \left[\sum_{j=3}^{2m} -a_{2,j} x_j^2 + x_j \left(b_{2,j} + \sum_{k=j+1}^{2m} d_{2,j,k} x_k \right) \right] \left(\prod_{k=3}^{2m} g_{2,k} x_k^{r_{2,k}} \right) \quad (\text{F15})
\end{aligned}$$

where the last equality results from following a similar simplification as was done following the x_1 integral and we define:

$$\begin{aligned}
a_{2,j} &:= a_{1,j} - \frac{d_{1,2,j}^2}{4a_{1,2}} \\
b_{2,j} &:= b_{1,j} + \frac{b_{1,2} d_{1,2,j}}{2a_{1,2}} \\
d_{2,j,k} &:= d_{1,j,k} + \frac{d_{1,2,j} d_{1,2,k}}{2a_{1,2}} \\
g_{2,k} &:= \frac{g_{1,k} d_{1,2,k}^{u_{2,k}}}{u_{2,k}!} \\
r_{2,k} &:= r_{1,k} + u_{2,k}. \quad (\text{F16})
\end{aligned}$$

The next $2m-2$ integrals can be evaluated iteratively following the same steps as above which results in the following closed form of the m -mode inner product:

$$\begin{aligned}
\langle F_{\mathbf{x}_1}^* | F_{\mathbf{x}_2}^* \rangle &= \frac{1}{\pi^m} \exp \left(C^{(1)*} + C^{(2)} + \sum_{j=1}^{2m} \frac{b_{j-1,j}^2}{4a_{j-1,j}} \right) \sum_{i_1+\dots+i_m=n} \sum_{j_1+\dots+j_m=n} \beta_{\mathbf{i}}^{(1)*} \beta_{\mathbf{j}}^{(2)} \\
&\times \sum_{\mathbf{p}=\mathbf{0}}^{\mathbf{i}} \sum_{\mathbf{q}=\mathbf{0}}^{\mathbf{j}} \prod_{\ell=1}^{2m-1} \left(\sum_{s_{\ell}=0}^{r_{\ell-1,\ell}} \frac{\gamma_{r_{\ell-1,\ell},s_{\ell}}}{a_{\ell-1,\ell}^{(r_{\ell-1,\ell}+s_{\ell}+1)/2}} \sum_{t_{\ell}=0}^{s_{\ell}} \frac{s_{\ell}!}{(s_{\ell}-t_{\ell})!} b_{\ell-1,\ell}^{s_{\ell}-t_{\ell}} \right. \\
&\times \sum_{u_{\ell,\ell+1}+\dots+u_{\ell,2m}=t_{\ell}} g_{\ell,\ell+1} \left. \right) \left(\sum_{s_{2m}=0}^{r_{2m-1,2m}} \frac{\gamma_{r_{2m-1,2m},s_{2m}}}{a_{2m-1,2m}^{(r_{2m-1,2m}+s_{2m}+1)/2}} b_{2m-1,2m}^{s_{2m}} \right) \quad (\text{F17})
\end{aligned}$$

where

$$\begin{aligned}
a_{i,j} &:= a_{i-1,j} - \frac{d_{i-1,i,j}^2}{4a_{i-1,i}} \\
b_{i,j} &:= b_{i-1,j} + \frac{b_{i-1,i}d_{i-1,i,j}}{2a_{i-1,i}} \\
d_{i,j,k} &:= d_{i-1,j,k} + \frac{d_{i-1,i,j}d_{i-1,i,k}}{2a_{i-1,i}} \\
g_{i,k} &:= \frac{g_{i-1,k}d_{i-1,i,k}^{u_{i,k}}}{u_{i,k}!} \\
r_{i,k} &:= r_{i-1,k} + u_{i,k}.
\end{aligned} \tag{F18}$$

are defined recursively and the $\gamma_{r,s}$'s are defined in Eq. (27). We note that this expression is still a product of Gaussian and a polynomial of degree $2n$.

Appendix G: Calculation of the Qudit Kernel

In this section we show the details of the calculation of the qudit kernel (Eq.(53)),
In the function representation, the inner product of two qudits is

$$\begin{aligned}
\langle F_1^*(z) | F_1^*(z) \rangle &= \frac{1}{\pi} \int_{z \in \mathbb{C}} dz^2 e^{-z^2} \left(\sum_{i=0}^{d-1} n_{d,i}^* \alpha_i^{(1)*} (z^*)^i \right) \left(\sum_{j=0}^{d-1} n_{d,j} \alpha_j^{(2)} z^j \right) \\
&= \frac{1}{\pi} \sum_{i=0}^{d-1} \sum_{j=0}^{d-1} n_{d,i}^* n_{d,j} \alpha_i^{(1)*} \alpha_j^{(2)} \int_{-\infty}^{\infty} dx \int_{-\infty}^{\infty} dy e^{-(x^2+y^2)} (x - iy)^i (x + iy)^j \\
&= \frac{1}{\pi} \sum_{i=0}^{d-1} \sum_{j=0}^{d-1} n_{d,i}^* n_{d,j} \alpha_i^{(1)*} \alpha_j^{(2)} \sum_{p=0}^i \sum_{q=0}^j \binom{i}{p} \binom{j}{q} (-i)^p (i)^q \left(\int_{-\infty}^{\infty} dy e^{-y^2} y^{p+q} \right) \\
&\quad \times \left(\int_{-\infty}^{\infty} dx e^{-x^2} x^{i+j-p-q} \right) \\
&= \frac{1}{\pi} \sum_{i=0}^{d-1} \sum_{j=0}^{d-1} n_{d,i}^* n_{d,j} \alpha_i^{(1)*} \alpha_j^{(2)} \sum_{p=0}^i \sum_{q=0}^j \binom{i}{p} \binom{j}{q} (-i)^p (i)^q \left(\frac{1 + (-1)^{p+q}}{2} \Gamma\left(\frac{1+p+q}{2}\right) \right) \\
&\quad \times \left(\frac{1 + (-1)^{i+j-p-q}}{2} \Gamma\left(\frac{1+i+j-p-q}{2}\right) \right) \\
&= \frac{1}{\pi} \sum_{i=0}^{d-1} \sum_{j=0}^{d-1} \frac{1 + (-1)^{i+j}}{2} n_{d,i}^* n_{d,j} \alpha_i^{(1)*} \alpha_j^{(2)} \sum_{p=0}^i \sum_{q=0}^j (-1)^q \binom{i}{p} \binom{j}{q} \cos\left(\frac{\pi(p+q)}{2}\right) \\
&\quad \times \Gamma\left(\frac{1+p+q}{2}\right) \Gamma\left(\frac{1+i+j-p-q}{2}\right)
\end{aligned} \tag{G1}$$

where each term the sum is zero unless both $(i+j)$ and $(p+q)$ are even. Now using the fact that

$$\Gamma\left(\frac{1}{2} + n\right) = \sqrt{\pi} \frac{(2n)!}{4^n n!} \tag{G2}$$

the qudit inner product becomes

$$\begin{aligned}
\langle F_1^*(z) | F_1^*(z) \rangle &= \frac{1}{\pi} \sum_{i=0}^{d-1} \sum_{j=0}^{d-1} \frac{1 + (-1)^{i+j}}{2} n_{d,i}^* n_{d,j} \alpha_i^{(1)*} \alpha_j^{(2)} \sum_{p=0}^i \sum_{q=0}^j (-1)^q \binom{i}{p} \binom{j}{q} \cos\left(\frac{\pi(p+q)}{2}\right) \\
&\quad \times \left(\sqrt{\pi} \frac{(p+q)!}{4^{(p+q)/2} (p+q)/2)!} \right) \left(\sqrt{\pi} \frac{(i+j-p-q)!}{4^{(i+j-p-q)/2} (i+j-p-q)/2)!} \right) \\
&= \sum_{i=0}^{d-1} \sum_{j=0}^{d-1} \frac{1 + (-1)^{i+j}}{2} \frac{1}{2^{(i+j)}} n_{d,i}^* n_{d,j} \alpha_i^{(1)*} \alpha_j^{(2)} \sum_{p=0}^i \sum_{q=0}^j (-1)^q \binom{i}{p} \binom{j}{q} \cos\left(\frac{\pi(p+q)}{2}\right) \\
&\quad \times \frac{(p+q)!}{(p+q)/2)!} \frac{(i+j-p-q)!}{(i+j-p-q)/2)!}.
\end{aligned} \tag{G3}$$

1. Calculation of the Qudit Kernel from the general multi-mode kernel

In this section, we calculate the qudit kernel from the general multi-mode kernel (Eq. (46)).

First we note that when $x = 0$

$$\sum_{j=0}^n \alpha_j x^j = \sum_{j=0}^n \alpha_j \delta_{j,0} = \alpha_0. \tag{G4}$$

Since a qudit can always be represented as a function of a single complex variable, we set $m = 1$. Additionally from Eq. (50) we find that

$$\begin{aligned}
a_{0,j} &= 1 \\
b_{0,j} &= 0 \\
d_{0,j,k} &= 0 \\
C^{(1)} &= C^{(2)} = 0
\end{aligned}$$

and by the recursion relations (Eq. (47))

$$\begin{aligned}
a_{i,j} &= 1 \\
b_{i,j} &= 0 \\
d_{i,j,k} &= 0.
\end{aligned}$$

Now the inner product becomes

$$\begin{aligned}
\langle F_1^*(z) | F_2^*(z) \rangle &= \frac{1}{\pi} \sum_{i=0}^n \sum_{j=0}^n \beta_i^{(1)*} \beta_j^{(2)} \sum_{p=0}^i \sum_{q=0}^j \sum_{s_1=0}^{r_{0,1}} \gamma_{r_{0,1},s_1} \sum_{t_1=0}^{s_1} \frac{s_1!}{(s_1-t_1)!} \delta_{t_1,s_1} g_{1,2} \sum_{s_2=0}^{r_{1,2}} \gamma_{r_{1,2},s_2} \delta_{s_2,0} \\
&= \frac{1}{\pi} \sum_{i=0}^n \sum_{j=0}^n \beta_i^{(1)*} \beta_j^{(2)} \sum_{p=0}^i \sum_{q=0}^j \sum_{s_1=0}^{r_{0,1}} \gamma_{r_{0,1},s_1} \sum_{t_1=0}^{s_1} \frac{s_1!}{(s_1-t_1)!} \delta_{t_1,s_1} \left(\frac{g_{0,2}}{t_1!} \delta_{t_1,0} \right) \sum_{s_2=0}^{r_{0,2}+t_1} \gamma_{r_{0,2}+t_1,s_2} \delta_{s_2,0} \\
&= \frac{1}{\pi} \sum_{i=0}^n \sum_{j=0}^n \beta_i^{(1)*} \beta_j^{(2)} \sum_{p=0}^i \sum_{q=0}^j \gamma_{r_{0,1},0} g_{0,2} \gamma_{r_{0,2},0} \\
&= \frac{1}{\pi} \sum_{i=0}^n \sum_{j=0}^n \beta_i^{(1)*} \beta_j^{(2)} \sum_{p=0}^i \sum_{q=0}^j \gamma_{p+q,0} \left(\binom{i}{p} \binom{j}{q} (-i)^p (i)^q \right) \gamma_{i+j-p-q,0}
\end{aligned} \tag{G5}$$

where in the second line, we substitute in the recursion relations for g and r (Eq. (48)) and in the fourth line we substitute in the initial values of g and r (Eq. (F7)).

From Eq. (27),

$$\begin{aligned}\gamma_{r,0} &= \begin{cases} \Gamma\left(\frac{1+r}{2}\right), & r \text{ even} \\ 0, & \text{otherwise} \end{cases} \\ &= \frac{1+(-1)^r}{2} \Gamma\left(\frac{1+r}{2}\right)\end{aligned}\tag{G6}$$

and so

$$\begin{aligned}\langle F_1^*(z) | F_2^*(z) \rangle &= \frac{1}{\pi} \sum_{i=0}^n \sum_{j=0}^n \beta_i^{(1)*} \beta_j^{(2)} \sum_{p=0}^i \sum_{q=0}^j \binom{i}{p} \binom{j}{q} (-i)^p (i)^q \\ &\quad \times \left(\frac{1+(-1)^{p+q}}{2} \Gamma\left(\frac{1+p+q}{2}\right) \right) \left(\frac{1+(-1)^{i+j-p-q}}{2} \Gamma\left(\frac{1+i+j-p-q}{2}\right) \right)\end{aligned}\tag{G7}$$

which matches the result from directly integrating the qudit inner product (Eq. (G1)) for $n = d - 1$ and $\beta_j = n_{d,j} \alpha_j$.